An-Najah National University

Faculty of Graduate Studies

UTILIZING MODIFIED KAOLINITE FOR PHENAZOPYRIDINE REMOVAL THROUGH ADSORPTION AND SUBSEQUENT THERMOLYSIS DECOMPOSITION

By

Sahar Marzouq Abdelrahman Salman

Supervisors

Prof. Ahed Zyoud

Dr. Derar Al-Smadi

This Thesis is Submitted in Partial Fulfillment of the Requirements for the Degree of Master of Chemistry, Faculty of Graduate Studies, An-Najah National University, Nablus - Palestine.

2024

UTILIZING MODIFIED KAOLINITE FOR PHENAZOPYRIDINE REMOVAL THROUGH ADSORPTION AND SUBSEQUENT THERMOLYSIS DECOMPOSITION

By

Sahar Marzouq Abdelrahman Salman

This Thesis was Defended Successfully on 21/11/2024 and approved by

Prof. Ahed Zyoud	
Supervisor	Signature
Dr. Derar Al-Smadi	
Co-Supervisor	Signature
Dr. Sami Makharza	
External Examiner	Signature
Prof. Othman Hamed	
Internal Examiner	Signature

Dedication

To my family, especially my parents, I dedicate this thesis with deepest gratitude for your unwavering support, love, and belief in me. Your constant encouragement has been my strength, and without your sacrifices, none of this would have been possible. I also take a moment to honor myself for the perseverance and resilience I have shown in the face of challenges and for continuing to push forward toward my goals. This journey is as much about growth and learning as it is about the love that binds us all.

.

Acknowledgements

I would first like to express my deepest gratitude to God, whose grace and blessings have been with me throughout this journey. It is through His guidance and support that I have been able to persevere, overcome challenges, and accomplish this significant milestone. I am truly thankful for the strength and wisdom granted to me during this time.

I would also like to extend my heartfelt thanks to my supervisor, Prof. Ahed Zyoud, whose insightful guidance and continuous support have been invaluable throughout this research. His expertise, patience, and encouragement have greatly contributed to the success of this work. I am equally grateful to my co-supervisor, Dr. Derar Al-Smadi, whose advice and constructive feedback have further enriched my research experience. I extend my gratitude to Dr. Samer Zyoud for his assistance with the XRD and SEM analysis. Additionally, I thank Shaher Zyoud for his role in the principal research idea and conceptualization

I am deeply grateful to my family especially my parents for their constant support, encouragement, and belief in me throughout this journey. Their love, patience, and sacrifices have been my greatest source of strength and motivation. This accomplishment would not have been possible without their unwavering presence by my side.

A special thank you to my colleagues, Ms. Nadeen Abbas and Ms. Yasmeen Hamdan, for their unwavering support, which has made this journey more enjoyable and productive. I am also deeply appreciative of Mr. Ameed Amerih, the research laboratory supervisor, for his technical assistance and for ensuring that all necessary resources were available throughout the experimental process.

Declaration

I, the undersigned, declare that I submitted the thesis entitled:

UTILIZING MODIFIED KAOLINITE FOR PHENAZOPYRIDINE REMOVAL THROUGH ADSORPTION AND SUBSEQUENT THERMOLYSIS DECOMPOSITION

I declare that the work provided in this thesis, unless otherwise referenced, is the researcher's own work, and has not been submitted elsewhere for any other degree or qualification.

Student's Name: **Sahar Marzouq Abdelrahman Salman**

Signature: 

Date: **21/11/2024**

List of Contents

Dedication III
Acknowledgements IV
Declaration V
List of Contents VI
List of Tables IX
List of Figures X
List of Appendices XI
Abstract XIII
Chapter One: Introduction 1
1.1 Background 1
1.2 Sources of water pollution 2
1.2.1 Dyes 2
1.2.2 Pharmaceuticals 5
1.3 Water treatment technologies 7
1.4 Adsorption process 8
1.5 Clay 10
1.5.1 Kaolinite 11
1.6 Adsorption isotherms 13
1.7 Objectives of the study 15
Chapter Two: Experimental, Instruments and Materials 16
2.1 Modification of kaolinite 17
2.2 The point of zero charge pH (pzc) 17
2.3 Phenazopyridine 18
2.3.1 Sample preparation and calibration curve 18
2.3.1.1 Preparation of stock solution and working solution 18
2.3.1.2 Preparation of standard solutions 18
2.3.1.3 Construction of the calibration curve 18
2.3.2 Effect of the concentration of adsorbate 19
2.3.3 Effect of the amount of adsorbent 19
2.3.4 Effect of pH 19
2.3.5 Effect of temperature 19
2.3.6 Recovery and reuse 20
2.3.6.1 Determination of the optimal thermolysis temperature 20

2.3.6.2 Decomposition of the sample 20
2.4 Methyl Orange 21
2.4.1 Sample preparation and calibration curve 21
2.4.1.1 Preparation of stock solution and working solution 21
2.4.1.2 Preparation of standard solutions 21
2.4.1.3 Construction of the calibration curve 21
2.4.2 Effect of the concentration of adsorbate 22
2.4.3 Effect of the amount of adsorbent 22
2.4.4 Effect of pH 22
2.4.5 Effect of temperature 22
2.4.6 Recovery and reuse 23
2.4.6.1 Determination of the optimal thermolysis temperature 23
2.4.6.2 Decomposition of the sample 23
2.5 Characterization 24
2.5.1 FT-IR 24
2.5.1.1 Phenazopyridine 24
2.5.1.2 Methyl orange 24
2.5.2 XRD and SEM 24
Chapter Three: Results and Discussions 25
3.1 Comparison between kaolinite and modified kaolinite 25
3.2 Modified kaolinite characterization 27
3.2.1 XRD characterization 27
3.2.2 SEM characterization 28
3.2.3 The point of zero charge pH (pzc) 29
3.3 Phenazopyridine 29
3.3.1 Formation of the calibration curve 29
3.3.2 Effect of the concentration of adsorbate 30
3.3.3 Effect of the amount of adsorbent 31
3.3.4 Effect of pH 33
3.3.5 Adsorption Isotherms 34
3.3.6 Adsorption kinetics 36
3.3.7 Effect of temperature 39
3.3.8 Determination of the activation energy 40
3.3.9 Recovery and reuse 41
3.3.9.1 TGA characterization 41

3.3.9.2 Reuse cycles 42
3.3.10 FT-IR characterization 42
3.4 Methyl orange 43
3.4.1 Formation of the calibration curve 43
3.4.2 Effect of the concentration of adsorbate 43
3.4.3 Effect of the amount of adsorbent 43
3.4.4 Effect of pH 44
3.4.5 Adsorption Isotherms 45
3.4.6 Adsorption kinetics 46
3.4.7 Effect of temperature 47
3.4.8 Determination of the activation energy 47
3.4.9 Recovery and reuse 48
3.4.9.1 TGA characterization 48
3.4.9.2 Reuse cycles 48
3.4.10 FT-IR characterization 49
3.5 Conclusion 49
3.6 Future work 50
List of Abbreviations 51
References 52
Appendices 61
الملخص ..... ب

List of Tables

Table 1.1: The specifications of MO 4
Table 1.2: The specifications of PhPy 6
Table 3.1: Langmuir and Freundlich isotherm parameters and correlation coefficients for PhPy adsorption onto modified kaolinite 36
Table 3.2: Pseudo first-order and pseudo second-order kinetic models and intra particle diffusion kinetic model parameters and correlation coefficients for PhPy adsorption onto modified kaolinite 39
Table 3.3: The calculations of activation energy for the adsorption of PhPy onto modified kaolinite at different temperatures 41
Table 3.4: Langmuir and Freundlich isotherm parameters and correlation coefficients for MO adsorption onto modified kaolinite. 45
Table 3.5: Pseudo first-order and pseudo second-order kinetic models, and intraparticle diffusion kinetic model parameters and correlation coefficients for MO adsorption onto modified kaolinite 46
Table 3.6: The calculations of activation energy for the adsorption of MO onto modified kaolinite at different temperatures 47

List of Figures

Figure 3.1: Comparison between kaolinite and modified kaolinite 26
Figure 3.2: XRD pattern of modified kaolinite 27
Figure 3.3: SEM image of modified kaolinite 28
Figure 3.4: Plot of Δ (pH) vs. initial pH for modified kaolinite. The intercept shows the value of pH(zcp) for the solid. The results were obtained at room temperature 29
Figure 3.5: Calibration curve of PhPy 30
Figure 3.6: Amounts of PhPy removed (ppm) over time under various conditions: 0.5 g/50 ml, 25 °C, 200 rpm, and pH = 5 for half an hr 31
Figure 3.7: Effect of adsorbent amount (g) on the removal efficiency of the PhPy 32
Figure 3.8: Effects of pH on the removal efficiency of PhPy 33
Figure 3.9: (a) Adsorption isotherms of PhPy onto modified kaolinite, (b) Langmuir isotherm, and (c) Freundlich isotherm 35
Figure 3.10: (a) Pseudo first-order, (b) Pseudo second-order, and (c) Intra particle diffusion 38

List of Appendices

Appendix A1: Figures 61
Figure A.1: Adsorption of PhPy on modified kaolinite at different temperatures, pH of 5, and shaking speed of 200 rpm for half an hour: (a) 0.2 g/50 mL for 30 ppm and (b) 0.5 g/50 mL for 60 ppm 61
Figure A.2: Plot of 1/T vs Ln k to determine the activation energy for the adsorption of PhPy on modified kaolinite 62
Figure A.3: TGA results of modified kaolinite and PhPy 62
Figure A.4: Stability of modified kaolinite after reuse, % removal of PhPy for the 4 reuse experiments 63
Figure A.5: FTIR spectra for PhPy adsorption onto modified kaolinite: (a) pure modified kaolinite, (b) PhPy (c) PhPy onto modified kaolinite (d) PhPy onto modified kaolinite after thermal decomposition at 600 °C 64
Figure A.6: Calibration curve of MO 65
Figure A.7: Amounts of MO removed (ppm) over time under various conditions, 0.5 g/50 mL, pH of 2, shaking speed of 200 rpm and 25 °C for half an hr 65
Figure A.8: Effect of the amount of adsorbent (g) on the removal efficiency of MO. Conditions, 50 mL of MO solution (50 ppm), solution pH of 2, shaking time = half an hour, shaking speed = 200 rpm, and 25 °C 66
Figure A.9: Effect of pH on the removal efficiency of MO. The conditions used were as follows: 50 mL of MO solution (50 ppm), shaking time is half an hour, amount of adsorbent is 0.5 g, shaking speed is 200 rpm, and 25 °C 66
Figure A.10: (a) Adsorption isotherms of MO onto modified kaolinite, (b) Langmuir isotherm, and (c) Freundlich isotherm. 67
Figure A.11: (a) Pseudo first-order, (b) Pseudo second-order, and (c) Intra particle diffusion 68
Figure A.12: Adsorption of MO on modified kaolinite at different temperatures, pH of 2, and shaking speed of 200 rpm for half an hour at 0.5 g/50 mL ... 69
Figure A.13: Plot of 1/T vs Ln k to determine the activation energy for the adsorption of MO on modified kaolinite 69
Figure A.14: TGA results of modified kaolinite and MO 70
Figure A.15: Stability of modified kaolinite after reuse, % removal of MO for the 4 reuse experiments 70

Figure A.16: FTIR spectra for MO adsorption onto modified kaolinite: (a) pure modified kaolinite, (b) MO (c) MO onto modified kaolinite (d) MO onto modified kaolinite after thermal decomposition at 600 °C..... 71

UTILIZING OF MODIFIED KAOLINITE FOR PHENAZOPYRIDINE REMOVAL THROUGH ADSORPTION AND SUBSEQUENT THERMOLYSIS DECOMPOSITION

By
Sahar Marzouq Abed Al-Rahman Salman
Supervisors
Prof. Ahed Zyoud
Dr. Derar Al-Smadi

Abstract

In this study, modified kaolinite was utilized as an adsorbent for the removal of phenazopyridine hydrochloride (PhPy) and methyl orange (MO) dyes from aqueous solutions. The effects of adsorbate concentration, adsorbent dosage, solution pH, and temperature were studied using UV-Vis. A decrease in concentration increased adsorption, which was influenced by the amount of modified kaolinite until equilibrium was reached. The ideal pH for PhPy adsorption was 5, while for MO, it was 2, with equilibrium achieved within 15 minutes. Adsorption decreased with increasing temperature, indicating exothermic behavior. Kinetic models were applied to describe the adsorption process, which followed pseudo-second-order kinetics for both dyes. Adsorption data fit the Langmuir isotherm model well, confirming monolayer adsorption. Activation energy was calculated, verifying that the adsorption process involved physical interactions.

Characterization of modified kaolinite was performed to understand its adsorption properties. X-ray diffraction (XRD) revealed changes in interlayer spacing, highlighting interactions between kaolinite and $ZnCl_2$. Scanning electron microscopy (SEM) showed increased surface roughness and porosity due to modification. Thermogravimetric analysis (TGA) confirmed the material's thermal stability and its ability to regenerate for four cycles at 600 °C without efficiency loss.

Fourier transform infrared (FT-IR) spectroscopy provided further insights into adsorption mechanisms, with spectral shifts indicating dye adsorption onto modified kaolinite. FT-IR also revealed functional group changes after thermal treatment, confirming the decomposition of PhPy and MO at 600 °C and successful regeneration of the adsorbent surface. The disappearance of organic functional group peaks validated the regeneration

process, ensuring the reusability of the modified kaolinite. The findings demonstrate the efficiency and reusability of modified kaolinite for dye removal from aqueous solutions, offering a sustainable approach to wastewater treatment.

Keywords: Modified kaolinite, Phenazopyridine hydrochloride, Methyl orange, Adsorption, Adsorbate, Adsorbent, Thermal decomposition

Chapter One
Introduction

1.1 Background

Water is one of the most important natural resources for the life of all living creatures and the continuation of life on Earth. This is proven in the Holy Qur'an, Surah Al-Anbiya'a, Ayah No. 30 (And We made from water every living thing) (1). Water constitutes 60% of the human body (2), and its importance within the body lies in the processes of digestion, construction, and renewal of cells (3). Water is also important in agriculture and industry in various fields (4). In short, water plays a fundamental and important role in all aspects of life.

Water covers (71%) of the Earth's surface and is represented by water from oceans, seas, rivers and lakes, but not all of it is available for use. Ninety-seven percent of it undrinkable (5). Two percent of it stored in lakes and glaciers and cannot be extracted, leaving only (1%) suitable for human consumption (6). This percentage is found in groundwater, lakes and rivers, but unfortunately, it is threatened by depletion (7).

Because only 1% of the water in the world is suitable for human use and this water is also prone to pollution, the world is facing major catastrophe, as one of the first sources of polluted water in general and groundwater in particular are agricultural fertilizers and pesticides (8), and factory waste and sewage leakage also occur.

A number of dangerous elements, including industrial dyes, heavy metals, waste pharmaceuticals, and organic contaminants, are contributing to increasing concerns regarding water quality problems. These contaminants enter groundwater, surface water, and even drinking water reserves, posing serious risks to important aquatic resources that support life and the balance of ecosystems. The various problems resulting from water contamination must be recognized and addressed to solve this critical issue (9, 10).

Many scientists and researchers have sought to purify water through several methods and techniques, including electrochemical technologies (11), the reverse osmosis process (12), photodegradation, adsorption by using different adsorbents (13, 14) and nanotechnology (15), but the main objective remains to find an effective and cheap method by using available materials. Therefore, we work and strive to find a simple,

inexpensive, easy, practical and environmentally friendly technology to effectively purify as much water as possible.

1.2 Sources of water pollution

The definition of water pollution is the exposure of oceans, seas, lakes, rivers and groundwater to pollutants that are harmful to the environment, humans and other living organisms (16). These pollutants change the qualities and properties of water, making it unfit for human use. There are many sources that pollute water, including human and animal waste, pesticides and fertilizers; urbanization, which includes heavy metals, oil and grease (17, 18); and factory waste, including dyes and pharmaceutical factories, which represent organic pollutants, which are among the most difficult types to treat and dispose of (19).

1.2.1 Dyes

Dyes are synthetic organic compounds whose main components are chromophores and auxochromes (20). These ingredients are usually used to add color to household furniture, rubber, fabrics, cosmetics, paper and leather. More than 700 thousand tons of dyes are produced annually, and according to research, the home furniture industry consumes approximately (60–70%) of the dyes produced (21).

Despite the use of dyes, their disposal still causes environmental pollution, as their disposal causes water pollution, which is highly dangerous because most dyes are extremely harmful, as they are prickly and carcinogenic (22) and are difficult to eliminate via usual methods such as coagulation, flocculation, and activated sludge (23). However, some modern methods, such as adsorption and photodegradation, work effectively to remove these dyes from water.

Dyes are usually classified according to their presence, whether they are manufactured or natural (24). They can also be classified according to the chromophore substance present, as they are classified into anthraquinone, nitro, nitroso, and azo dyes. Azo dyes are among the most famous types of dyes used and constitute (70%) of manufactured dyes (23).

Azo dyes are a notable type of dye distinguished by the presence of one or more of the azo groups [R_1-N=N-R_2] attached to the aromatic ring (23). It is the most widespread type among dyes and is included in many industries, such as cosmetics, leather, paper, and

fabrics, owing to its multiplicity of colors and its stable color, which is resistant to changes such as exposure to sunlight and heat.

Despite all the uses of this type of dye and its advantages, leakage into water and contamination are major disasters since it is capable of disintegrating into aromatic amines. This substance is very toxic, carcinogenic, and mutagenic (25). It is not disposed of by traditional methods such as activated sludge or coagulation, but it requires modern methods because it poses a great danger to humans and marine organisms (26).

Azo dyes can be classified according to their color. There are yellow azo dyes, such as tartrazine and sunset yellow, and red dyes, such as Allura Red, and blue dyes, such as Brilliant Blue (27). Azo dyes can also be distributed toward the number of azo groups, as they may be monoazos, such as phenazopyridine; they may be diazos, such as red ponceau S; triazos, such as direct blue 71; and poliazos, such as direct red 80 (28).

Methyl orange (MO) which will be used as a water dyes contaminant model is a synthetic dye belonging to the azo class of dyes and is a pH indicator used in titrations because its color
changes from red to yellow over a pH range of 3--7 (29). Azo dyes such as MO are usually used in different industries, such as textiles, food, and pharmaceuticals. The chemical structure of MO contains a sulfonic acid group, which makes it water soluble, and its ionization at different pH values is responsible for the observed color change during titrations (30). The specifications of MO are listed in Table 1.1

Table 1.1

The specifications of MO

Name	Methyl orange
Chemical structure	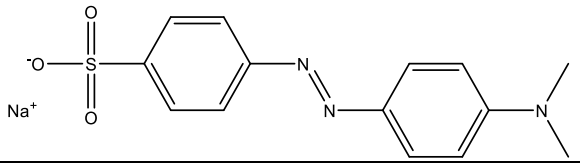
IUPAC Name	sodium;4-[[4-(dimethylamino)phenyl[diazenyl]benzenesulfonate
Solubility in water	Soluble
Molecular weight	327.34 g/mol
Chemical formula	$C_{14}H_{14}N_3NaO_3S$
Color	Acidic medium: Red Basic medium: Yellow
λ_{max}	464 nm
CAS	547-58-0

The color of MO changes with pH because of the protonation and deprotonation of its azo bond, which affects the conjugated pi–electron system of the molecule. In acidic conditions, MO is protonated, causing the molecule to absorb light in a way that makes it appear red. When the pH increases and becomes more basic, the dye is deprotonated, and the color shifts to yellow (31). This attitude has been confirmed in different studies that have reported the interaction of azo dyes with proton donors and acceptors (32).

Treating azo dyes such as MO is essential because of their danger to living organisms and their resistance to biodegradation (32). Therefore, there are many ways to eliminate these compounds, such as photodegradation and adsorption. Photodegradation is defined as breaking the dye by means of light alone or with the use of catalysts. The latter method uses a substance that has the ability to adsorb. For example, activated carbon or clay absorbs dye from a solution and removes it (33).

1.2.2 Pharmaceuticals

Pharmaceutical drugs are among the most useful substances invented by researchers for humanity. They are used to prevent and treat diseases and take care of health (34). They are made resistant to disintegration and changes due to ambient conditions. As a result, they are stable and harmless within the human body. However, this has a negative impact when they are disposed of incorrectly, contaminating water and making them resistant to photodegradation and traditional removal methods (35).

Pharmaceuticals are divided into several types. The first type is analgesics, which are used to relieve pain. The most famous examples are nonsteroidal anti-inflammatory drugs (NSAIDs), such as aspirin and ibuprofen (35). The second type is antibiotics, which are used to eliminate bacteria and fungi (36). The third type is hormones, which are used to treat the same hormones inside the body, such as synthetic estrogen (37), and the last type is psychiatry, which is used to treat depression (34).

Analgesics or painkillers are usually used to relieve pain and are the most widely used medications. Common examples include diclofenac, ibuprofen, and aspirin (35). Owing to their widespread use, this has led to their leakage into ground and surface water because the body removes their remains through urine, so they seep into the water and pollute it (38).

Various studies have shown that the presence of painkillers, even at very low concentrations, leads to great harm to marine creatures. Schwaiger et al. reported that diclofenac affects the growth of fish and that ibuprofen affects their production (39, 40); in the long run, this leads to extinction and disruption of the biological system. Additionally, the presence of analgesics and their access to drinking water poses a great danger. It is harmful to human health, as it causes great harm to the body, as it is difficult to eliminate and remove from water (41).

Phenazopyridine hydrochloride (PhPy) which will be used as a water pharmaceuticals contaminant model is a synthetic organic compound from the class of azo dyes used to combat pain and burn in the urinary tract (42). It is a brownish-red powder that is soluble in water. It is acidic and is not significantly affected by differences in pH. It can be taken with antibiotics to reduce the symptoms of the disease, but it does not treat the disease, reduces symptoms and is taken for a short period. The specifications of PhPy are listed in Table 1.2

Table 1.2

The specifications of PhPy

Name	Phenazopyridine hydrochloride
Chemical structure	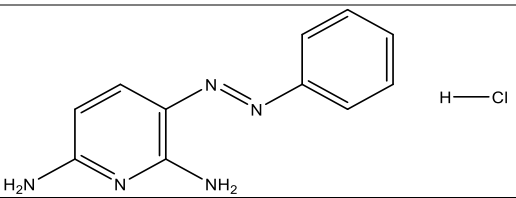
IUPAC Name	3-phenyldiazenylpyridine-2,6-diamine; hydrochloride
Solubility in water	Soluble
Molecular weight	249.7 g/mol
Chemical formula	$C_{11}H_{11}N_5.HCl$
Color	High concentration: Red Low concentration: Yellow
λ_{max}	425 nm
Color index of PhPy	16230
CAS	94-78-0

PhPy consists of a phenylazo group linked to a pyridine ring, making it unprepared for metabolic degradation and raising concerns about its environmental effects when it is excreted unchanged or as a metabolite (43).

PhPy causes several side effects, including urine becoming reddish-orange in color. This is not a cause for concern because it is not harmful, but it only indicates the presence of the drug inside the human body, but it causes other symptoms such as headache and stomach upset when taken without food. One of the characteristics of PhPy is that if it touches a surface, this surface gains a brownish red color. (44).

1.3 Water treatment technologies

The preservation of natural resources has become a basic requirement. Hence, much attention has been given to recycling these resources, including water treatment, as water pollution has become a major disaster affecting the entire world (45).

Water pollution with dyes or pharmaceuticals that are incorrectly disposed of from factories is a complex problem facing researchers in the field of water purification. These organic materials can decompose into other toxic and carcinogenic substances, which are difficult to eliminate via traditional methods such as coagulation, activated sludge, or sedimentation. These methods have proven ineffective, but modern methods, such as the advanced oxidation process (AOP), bioremediation, adsorption, and membrane filtration, have yielded promising results in the treatment process (46).

Bioremediation is one of the techniques utilized in water treatment, where microorganisms such as bacteria or fungi are used to break down organic compounds such as dyes into compounds that are easy to dispose of and are nontoxic. This method is inexpensive and environmentally friendly, but caution and precision are needed when dealing with the microorganisms used to ensure effectiveness (47).

Membrane filtration techniques are used in water treatment. These methods are similar to reverse osmosis and nanofiltration and are usually used to separate dyes by their size or charge; however, the challenge in this method remains the type of membrane and its efficiency, as this method requires an inexpensive, high-quality membrane to yield good results (48).

The AOP includes ozone, hydrogen peroxide, and ultraviolet light. This process produces radical hydroxyl groups that oxidize and breakdown organic compounds, which are used to break down and decompose organic compounds such as dyes into harmless, nontoxic compounds. It is also used to break down pharmaceuticals into noncarcinogenic compounds. Activated carbon can be added, which helps adsorb pharmaceuticals very effectively and completely removes them from water (49).

1.4 Adsorption process

Adsorption involves the transfer of molecules from gas, liquid, or dissolved solids and their adhesion to the surface of a liquid or solid substance to form a new atomic or molecular film (14). This process plays an important role in separating gases, treating water, and adsorbing to catalysts and can be divided into two types: chemical adsorption, or chemisorption, physical adsorption, or physisorption (50).

Physisorption is represented by the formation of van der Waals forces between the surface and molecules without any change in the adsorbent or adsorbate, such as the adsorption of ions onto a charged surface by electrostatic forces, which is known as electrostatic adsorption in water treatment processes (51).

On the other hand, chemisorption involves the formalization of a strong chemical bond between the surface and a molecule, which results in a significant change in the adsorbent or adsorbate, such as in the adsorption of diatomic gases, such as O_2 and H_2. The bond in the adsorbate breaks, leading to the formation of a new bond with the adsorbent; this process is called dissociative chemisorption (52). Ion exchange is also a type of adsorption that involves the exchange of ions between the adsorbent and adsorbate (53).

Adsorption plays an important role in the catalyst area. It works to adsorb the reacting molecules on the catalyst, which increases the reaction rate, such as the platinum catalyst used in car converters, which works to convert harmful gases in the air, such as carbon monoxide (CO) and nitrogen oxide gases (NO_x), into less harmful compounds (54).

The adsorption process strongly affects the removal of dangerous gases and volatile organic materials from the air. The most famous materials used to purify air are zeolites and metal–organic frameworks (MOFs). The latter has proven effective in eliminating carbon dioxide (CO_2) from the air because of its large surface area (55).

In water treatment, adsorption has an apparent effective role in eliminating pollutants such as organic pollutants and heavy metals. One of the most famous materials used is activated carbon, which works to adsorb pollutants because of its large surface area, which can be developed through the oxidation process (56); however, when activated carbon is disposed of, it will pollute the environment again because it is difficult to reuse (57). Other materials used in adsorption include various types of clay, such as

montmorillonite, kaolinite, zeolite, bentonite, and natural clay. These materials have a variety of benefits, including their fundamental abundance in the environment, cost-effectiveness, and ecological compatibility. Their demonstrated efficacy as adsorption agents for many different kinds of aquatic pollutants, including organic chemicals, is a major breakthrough for permanent pollution reduction (58).

More recent research has focused on the advantages of the combination of kaolin and montmorillonite. For application in natural resource applications, a theoretical study on methane adsorption at the silica–kaolinite interface was performed by Onawole et al. in 2021. Although this research is primarily concerned with shale gas exploration, it also highlights the potential of kaolin-based materials in challenging adsorption procedures (59).

Natural clays, which are made up of multiple clay minerals mixed together, provide unique advantages for adsorption applications. In their study of kaolin adsorption sites from 1976, Armstrong and Clarke highlighted the importance of the mineral composition of clay to optimize adsorption procedures. This study highlighted the importance of how various clay minerals interact with one another in natural clay matrices (60).

The understanding of adsorption mechanisms in clay minerals has benefited significantly from theoretical studies in addition to experiments. Gaines Jr. Thomas (1953) established a theoretical framework for investigating the adsorption of ions and molecules on clay surfaces by developing the thermodynamic principles of exchange adsorption on clay minerals (61). This important research provides a foundation for additional studies on clay mineral adsorption. For the purpose of modeling the adsorption of phosphate on hematite, kaolinite, and kaolinite-hematite systems, Ioannou and Dimirkou (1997) suggested a constant capacitance model (62). By considering different clay mineral compositions, our modeling technique improves our capacity to forecast and optimize phosphate removal from water.

The reviewed literature provides a comprehensive review of the various applications of natural clays, especially kaolin, and clay minerals, such as kaolinite and montmorillonite, in adsorption techniques for the elimination of different water pollutants. The experiments discussed here show how effective these materials may be in purifying wastewater, with applications ranging from the elimination of pharmaceutical pollutants to the removal of synthetic dyes.

1.5 Clay

Clay is natural rock with fine grains or soil materials that are plastic when wet with water because of the presence of minerals in their composition. Clay consists mainly of phyllosilicate, which contains a quantity of water. The most famous types of clay are kaolinite, illite, and montmorillonite (63).

The clay consists of layers of aluminum and silicon oxides, which are in the form of sheets that are held together by water molecules and various cations. This composition endows the clays with distinctive properties, such as swelling and shrinkage, which play a decisive and important role in its applications (64).

Clay has multiple important roles. The first of these roles is in agriculture, where clay can improve the structure of the soil. An example of this is bentonite, which helps increase soil fertility and reclamation (64). It has other distinct roles in geotechnical and environmental engineering, as it is an effective element for combating pollution, especially in water, where it can eliminate heavy metals and organic materials from polluted water because of its large surface area. It can also be used in landfills as a barrier to prevent the leakage of pollutants into groundwater (63).

In addition to the previous roles, clay is added to polymer compounds to enhance their mechanical properties and as catalysts in chemical reactions and drug delivery systems in the delivery of biomedical drugs. This is due to recent developments and research in nanoscience, where nano clay, which consists of clay granules with nanoscopic dimensions and improved properties, has been developed, as it has increased surface area and interactivity (65).

Clay usually requires modifications to improve their performance for specific applications, such as adsorption, catalysis, and environmental remediation. Different modification methods have been developed to enhance the surface properties, pore structure, and chemical reactivity of clays (66). These modifications generally include physical, chemical, or thermal treatments.

1.5.1 Kaolinite

Kaolinite is an industrial mineral with the chemical formula $Al_2Si_2O_5(OH)_4$ and is a clay mineral. Its basic unit is a layered silicate mineral with one tetrahedral layer of silica bonded through the same oxygen to one octahedral sheet of alumina. When this unit is repeated, kaolinite acquires its characteristics and its crystalline structure. Its distinctive properties make it an important metal in the ceramic, paper and refractory industries (67).

Furthermore, kaolinite has a low ability to shrink and exchange cations. These properties are the result of the structure and composition of kaolinite, where the strong hydrogen bonding between the layers prevents the intrusion of water or other molecules, which stabilizes its structure under different environmental conditions. This is one of the important properties of kaolinite (67).

Kaolinite is used in the paper industry, where it functions as a coating material to improve the smoothness, brightness, and printability of the paper. This is due to the size of the fine particles and the lamellar shape of kaolinite, which allows it to cover the largest area and achieve the best smoothness. It also has chemical inertness that helps prevent unwanted reactions. This is the primary use of kaolinite (68).

Kaolinite is invaluable in the ceramic industry, as it can maintain its shape during firing and contributes to the flexibility of the ceramic body, which makes it a major component in the production of porcelain. Kaolinite contains alumina and silica, which are necessary to form mullite. This is a crucial stage in the production of ceramic materials that contributes to thermal stability and enhances strength (69).

Owing to its high melting point and resistance to thermal shock, refractory industries make use of kaolinite. Kaolinite-based refractories are used in the linings of furnaces and other industrial equipment that has high temperatures. This is due to its ability to withstand very high temperatures without melting or decomposing. This ensures very high efficiency and continued use of the product without any damage (70).

Kaolinite is also used in modern applications, as nanograins of kaolinite can be added to polymer compounds to improve their thermal properties and mechanical strength. In addition, it has geochemical and pedological roles. It is one of the products of tropical

and subtropical soil weathering, as it works to improve soil properties such as structure, fill retention, and fertility (70).

Moreover, it has medical value, as Müller AS et al. have proven that it has potential in drug delivery systems, where its biocompatibility, ability to adsorb, and ability to release drugs are beneficial. Research related to the role of kaolinite in the medical field is still in its initial stage, but the initial results are promising (71).

In addition, it has adsorbent properties that make it environmentally friendly, as it is effective in removing pollutants from water and soil, as it can adsorb organic pollutants, dyes and heavy metals. This is due to the surface chemistry of kaolinite, which plays an important role in addition to its charge and surface area (71). The adsorption and removal of dyes from polluted water play prominent roles in kaolinite because of its surface area and porosity, which play important roles in capturing dye parts through electrostatic interactions and hydrogen bonding (72).

There are many examples of kaolinite adsorption dyes, and the natural clay mineral kaolin has drawn much interest as an adsorbent for removing water contaminants. In their study from 2022, Dadebo and Obura focused on the adsorption of Acid Red 88 onto kaolinite clay to remove it from aqueous solutions. These findings highlight the importance of treating textile industry effluents by demonstrating the significant adsorption potential of kaolin-based materials in removing synthetic dyes from water (73).

The ability of kaolin-based materials to successfully adsorb organic dyes was demonstrated by Ghosh and Bhattacharyya (2002) in a related study that examined the adsorption of methylene blue on kaolinite. Insightful information about the interactions of dyes with kaolin surfaces was provided in this study, along with clear explanations of the adsorption process (74). A. Virmonses et al. 2009 examined the affinity of three Australian kaolin samples for the common azo pigment Congo red (75). Research has shown that kaolin from different regions can be used to purify water. This potential was made apparent by variations in the adsorption capacities caused by variations in the mineral composition and structure.

Onyekweli examined the adsorptive properties of kaolin in their 2003 study with the hope of using it to filter drugs out of contaminated water. Research has revealed that kaolin has

numerous inventive uses in addition to its conventional use for purifying water containing pharmaceutical impurities (76).

1.6 Adsorption isotherms

Adsorption isotherms depict how adsorbent materials react with absorbable materials through graphical representations. They applied data obtained from the adsorption process at constant temperature and pH and provided precise specifications about the nature of the interaction between adsorbent molecules and the adsorbate surface and described the efficiency of adsorption processes and the capacity of adsorbent materials. The most famous models are the Langmuir and Freundlich models, which provide the mechanism of the adsorption process, as each of them gives a different concept and framework for the adsorption process grounded in different assumptions and criteria (77).

To obtain a relationship of the isotherm of adsorption between the amount of adsorbate per unit of adsorbent (q_e) and the equilibrium concentration of the solution after adsorption (C_e), the experimental data gained from adsorption experiments are addressed through several equations and relationships.

There are two common isothermal models: the Langmuir and Freundlich isothermal models. These isotherms are linked to the adsorbate per unit mass of the adsorbent (q_e) and to the equilibrium concentration adsorbed in solution after the adsorption process (C_e) according to the following equations: (78, 79)

$$q_e = \frac{C_o - C_e}{W} V \quad (1)$$

$$q_e = \frac{C_o - C_t}{W} V \quad (2)$$

where C_o, C_t, and C_e (mg/L) represent the initial and equilibrium adsorbate concentrations, t represents time, V (L) represents the volume of solution, and W (g) represents the solution adsorbent concentration.

Each model is built upon a set of propositions that fundamentally provide an idea about the adsorption mechanism. The correlation coefficient (R^2) was used to determine the most appropriate isotherm model; hence, the experimental data were analyzed via two renowned models, the Langmuir and Freundlich isotherm models.

The Langmuir isotherm, suggested by Irving Langmuir in 1918, was established on the basis of the postulation of single-layer adsorption on a homogeneous surface with a restricted number of corresponding places. When a site is filled, no supplementary adsorption can occur at that location (78). This model is represented by the following equation:

$$q_e = \frac{Q_o b C_e}{1 + b C_e} \tag{3}$$

Langmuir adsorption parameters are commonly resolved by converting the Langmuir equation into a linear form:

$$\frac{C_e}{q_e} = \frac{1}{b Q_o} + \frac{C_e}{Q_o} \tag{4}$$

where:

C_e = the concentration of adsorbate at equilibrium (mg/L)

q_e = the amount adsorbed per gram of adsorbent at equilibrium (mg/g).

Q_o = maximum monolayer coverage capacity constant at equilibrium (mg/g)

b = Langmuir isotherm constant related to the affinity of adsorption (L/mg).

The Freundlich isotherm is an experimental model that characterizes adsorption on heterogeneous surfaces with unequal apportionment of the heat of adsorption above the surface. In contrast to the Langmuir model, monolayer formation is not assumed. The Freundlich isotherm is not appropriate at very high pressures, but it is much more accurate than the Langmuir isotherm for intermediate pressures. The Freundlich isotherm is represented by the following equation:(78)

$$q_e = K_f C_e^{\frac{1}{n}} \tag{5}$$

where K_f (L/mg) and 1/n are the Freundlich adsorption constants. Eq. (5) can be rearranged as follows:

$$log\ q_e = log\ K_f + \frac{1}{n} log\ C_e \tag{6}$$

where:

q_e = the adsorbate mass per unit adsorbent mass (mg/g)

C_e = the remaining equilibrium concentration of the adsorbate (mg/L)

K_f = the Freundlich constant related to the adsorption capacity of the adsorbent (mg/g) $(mg/L)^{1/n}$).

(1/n) = the heterogeneity of the surface.

Hence, a plot of log q_e vs Log C_e gives a slope of 1/n and an intercept = log K_f. A smaller slope value indicates a more heterogeneous surface. A higher K_f value indicates the highest adsorption capacity, and the value of (1/n) determines whether the adsorption process is favorable. If (1/n) is lower than 1, Langmuir adsorption is favorable, whereas Freundlich adsorption occurs if (1/n) is greater than 1. This flexibility permits the Freundlich isotherm modeling of adsorption processes that do not fit the postulation of the Langmuir isotherm, making it especially beneficial for industrial and natural systems where surface heterogeneity is predominant (78).

1.7 Objectives of the study

Our main objectives in this study are to gain a comprehensive understanding of adsorption mechanisms, enhance clay-based adsorbents, and look into novel applications for addressing new water pollution problems by utilizing the unique properties of natural clays and clay minerals. Also, to provide insight into the potential of modified kaolinite as an effective adsorbent for the removal of phenazopyridine and methyl orange from water sources, followed by the subsequent thermal decomposition of the adsorbed phenazopyridine and methyl orange. Because of the thermal stability of modified kaolinite at temperatures above 1000 °C, regeneration by thermal decomposition of the molecules of organic contaminants that have been adsorbed into safe products such as CO_2 and H_2O to reuse the modified kaolinite repeatedly is possible, with versatility extending beyond pharmaceuticals and dyes to remove various organic contaminants from water. Further investigations into modified clay composites or alternative clay derivatives for related applications are also possible.

Additionally, studying the impact of different parameters, such as the amount of adsorbent, different concentrations of the solvent, solution pH, and temperature, on the adsorptive removal of the dye on modified kaolinite.

Chapter Two

Experimental, Instruments and Materials

Most of the chemicals used in this study, including kaolinite, phenazopyridine hydrochloride, methyl orange, NaCl, and $ZnCl_2$, were purchased from Sigma Aldrich Chemical Company. HCl and NaOH were purchased from CS Chemical Company. All the solid samples in this study were weighed with an MRC analytical balance Advent. For organic contamination, PhPy and MO were chosen as a model. On the other hand, modified kaolinite was chosen as the adsorbent.

For PhPy, batch adsorption experiments were executed by using 100 mL urine cups, each containing 50 mL of PhPy solution with an elementary concentration ranging from 20–80 ppm and a pH of 5, with a specified amount of modified kaolinite. The urine cups were tightly closed and shaken at 200 rpm at 25 °C for half an hour by using a Lab Tech water bath and shaker LSB-0. The pH was adjusted via a JENWAY model:35 pH meter, and the contaminated modified kaolinite was detached from the treated solution via LAB TRON LLS-A12 centrifuge in all the experiments. The supernatant was subsequently decanted, and the concentration was measured via UV-Spectrophotometry (UV–Vis SHIMADZU UV-1800). The contaminated modified kaolinite was collected and thermally decomposed via the MRC Bench Top Muffle Furnace up to 600 °C and then reused for four cycles.

For MO, batch adsorption experiments were executed by using 100 mL urine cups, each containing 50 mL of MO solution with an elementary concentration ranging from 10–70 ppm and a pH of 2, with a specified amount of modified kaolinite. The urine cups were tightly closed and shaken at 200 rpm at 25 °C for half an hour by using a Lab Tech water bath and shaker LSB-0. The pH was adjusted via a JENWAY model:35 pH meter, and the polluted kaolinite was detached from the treated solution via an LAB TRON LLS-A12 centrifuge in all the experiments. The supernatant was subsequently decanted, and the concentration was measured via UV-Spectrophotometry (UV–Vis SHIMADZU UV-1800). The separated contaminated modified kaolinite was collected and thermally decomposed by using an MRC Bench Top Muffle Furnace up to 600 °C and then reused for four cycles.

The modified kaolinite samples were characterized via PANalytical X'Pert PRO X-ray diffractometer (XRD) equipped with CuKα (1= 1.5418 Å) and Jeol-EO Scanning Electron

Microscopy (SEM) in AUE. The modified kaolinite, PhPy, MO, and contaminated modified kaolinite samples were characterized by Thermo Scientific Nicolet iS5 FT-IR at An-Najah National University in Palestine. PhPy, MO and modified kaolinite samples were characterized via SANAF TGA at An-Najah National University.

The experimental section of this study is divided into two parts. The first is the adsorption process, which includes adsorption experiments with different parameters, such as different concentrations of adsorbate and adsorbent, different pH values, and different temperatures. The second part includes reusing the contaminated modified kaolinite several times to test its efficiency and reusability.

2.1 Modification of kaolinite

A 100 g of fresh kaolinite was calcined at 600 °C for six hours. After that, the calcined kaolinite was soaked in 0.08 M $ZnCl_2$ solution for 6 hours with stirring. The kaolinite was subsequently dried in an oven at 80 °C for one hour (80).

2.2 The point of zero charge pH (pzc)

To prepare a 0.01 M solution of sodium chloride (NaCl), 0.29 g of NaCl was weighed. The mixture was transferred to a 500 mL volumetric flask. Then, distilled water was gradually added to the flask, ensuring that the water level approached the calibration mark on the flask. The flask was subsequently closed with a stopper. Finally, the flask was shaken vigorously to ensure that the NaCl dissolved completely and that the solution became homogeneous.

To prepare the samples, 50 mL of a 0.01 M NaCl solution was measured via a graduated cylinder. The solution was transferred into six separate glass bottles. Then, the initial pH was adjusted by using diluted solutions of HCl and NaOH for each solution to specific values: 2, 4, 6, 8, 10 and 12. After that, 0.1 g of modified kaolinite was added to each bottle. The bottles were then closed tightly with their caps. The bottles were placed on a shaker set to 200 rpm, and a constant temperature of 25 °C was maintained. The mixture was allowed to shake for 24 hours to ensure total mixing. After that, the final pH of each solution was measured to resolve any variation that may have occurred (81).

2.3 Phenazopyridine

2.3.1 Sample preparation and calibration curve

2.3.1.1 Preparation of stock solution and working solution

To prepare a 1000 ppm PhPy stock solution, 1 g of PhPy was weighed accurately and placed inside a 1000 mL volumetric flask, distilled water was added gently until it reached the mark, and the volume was adjusted. Then, the sealed volumetric flask was sonicated in a digital ultrasonic bath for 5 min until all the PhPy dissolved and the solution became clear.

For preparation of the working solution, 50 mL of stock solution was transferred into a 500 mL volumetric flask by using a pipette. The distilled water was subsequently added until the volume was adjusted, and the flask was subsequently closed and shaken vigorously until it became a homogenous solution with a 100 ppm concentration.

2.3.1.2 Preparation of standard solutions

In seven 100 mL volumetric flasks, 5, 10, 20, 30, 40, 60 and 80 mL were transferred from the working solution by pipette to prepare 5, 10, 20, 30, 40, 60 and 80 ppm solutions, respectively. Each flask was filled with distilled water to the mark, followed by vigorous shaking until a clear and homogenous solution formed.

2.3.1.3 Construction of the calibration curve

A calibration curve represents the relationship between the concentration of standard solutions and their absorbance at a specific wavelength, usually the maximum absorbance wavelength (λ max). In this study, a calibration curve was established using standard solutions with concentrations of 5, 10, 20, 30, and 40 ppm. These specific concentrations were chosen to ensure accurate and reliable measurements. Higher concentrations were excluded from the calibration curve because of their tendency to introduce errors into the results. At higher concentrations, deviations from Beer's law can occur, resulting in nonlinear and inaccurate absorbance readings (82). After the adsorption process was complete, the PhPy samples were analyzed, and their concentrations were resolved via the equation derived from the calibration curve.

2.3.2 Effect of the concentration of adsorbate

After the λ max was determined, 50 ml from 20, 30, 40, 60, and 80 ppm solutions were transferred to four urine cups by using a graduated cylinder. Then, 0.5 g of modified kaolinite was added, which was weighed carefully for each cup at a pH of 5. All the cups were then tightly closed and shaken at 200 rpm and 25 °C for half an hour. Each 5-minute portion from each cup was taken, the contaminated modified kaolinite was separated by centrifugation at 4000 rpm for 6 minutes, and the treated solution was analyzed via UV–Vis.

2.3.3 Effect of the amount of adsorbent

To prepare the samples, 0.1, 0.2, 0.3, 0.4, 0.5, and 0.6 g of modified kaolinite were weighed and transferred into twelve urine cups. Subsequently, 50 mL of 60 ppm solution was added by using a graduated cylinder for the first six and 50 mL of 30 ppm for the other, at a pH of 5. Next, the cups were closed and shaken at 200 rpm and 25 °C for half an hour. Each 5-minute portion from each sample was analyzed via UV–Vis at λmax = 425 nanometers.

2.3.4 Effect of pH

In this experiment, the effect of changing the pH was evaluated by varying the pH from 3 to 11. Each sample was prepared by weighing 0.5 g of modified kaolinite and placing it inside a urine cup, followed by the addition of 50 mL of 60 ppm solution, and 0.2 g of 30 ppm solution was used. The pH was subsequently adjusted by using diluted solutions of HCl and NaOH, after which the samples were closed and shaken for half an hour at 200 rpm and 25 °C. Five-minute portions from each sample were taken. After that, the supernatant was analyzed.

2.3.5 Effect of temperature

In this work, the process was carried out at four different temperatures: 17.5, 25, 32.5, and 40 °C. To prepare the samples, 0.5 g of modified kaolinite was placed in four urine cups, 50 mL of 60 ppm solution was added to each cup, and the process was repeated for 30 ppm, but 0.2 g was used instead of 0.5 g. The cups were subsequently tightly closed. All the samples were shaken at 200 rpm and a specific temperature for half an hour. Each 5-minute portion from each sample was removed, and the treated solution was analyzed.

2.3.6 Recovery and reuse

2.3.6.1 Determination of the optimal thermolysis temperature

To determine the optimal temperature for reusing the composite, a portion of the PhPy was analyzed via thermogravimetric analysis (TGA) over a period of two hours. This analysis aimed to identify the temperature at which the PhPy underwent complete decomposition. By gradually heating the sample and monitoring weight loss, TGA provided insights into the thermal stability of the PhPy and pinpointed the specific temperature range where decomposition occurs (83).

2.3.6.2 Decomposition of the sample

After the adsorption process was completed, the contaminated modified kaolinite was collected. The sample was designated and placed in a crucible and subjected to thermal decomposition at 600 °C for one hour. After decomposition, the treated modified kaolinite was allowed to cool to room temperature.

Once the optimal thermolysis temperature was determined and sample was prepared, the first cycle was carried out with careful precision. First, 0.5 g of modified kaolinite, which had been heated at 600 °C, was weighed. This was followed by the addition of 50 mL of a 60 ppm solution. The mixture was then shaken for half an hour at a speed of 200 rpm, a pH of 5 and a temperature of 25 °C. After that, the contaminated modified kaolinite was collected for further treatment. The collected modified kaolinite underwent thermal decomposition at 600 °C for half an hour and then allowed to cool at room temperature. The previous step was meticulously repeated for each subsequent cycle to maintain consistency and accuracy in the experimental procedure.

2.4 Methyl Orange

2.4.1 Sample preparation and calibration curve

2.4.1.1 Preparation of stock solution and working solution

To prepare a 1000 ppm MO stock solution, 1 g of MO was weighed accurately and placed inside a 1000 mL volumetric flask, distilled water was added gently until it reached the mark, and the volume was adjusted. Then, the sealed volumetric flask was sonicated in a digital ultrasonic bath for 5 min until all the MO dissolved and the solution became clear.

For the preparation of the working solution, 50 mL of the stock solution was measured using a pipette and transferred into a 500 mL volumetric flask. Distilled water was added to reach the desired volume, and the flask was sealed and shaken thoroughly to ensure the solution was uniform, yielding a concentration of 100 ppm.

2.4.1.2 Preparation of standard solutions

To prepare solutions with concentrations of 10, 20, 30, 40, 50, and 70 ppm, 10, 20, 30, 40, 50, and 70 mL of the working solution were pipetted into seven 100 mL volumetric flasks, respectively. Distilled water was added to each flask up to the calibration mark, and the contents were shaken thoroughly to ensure the formation of a clear and uniform solution.

2.4.1.3 Construction of the calibration curve

A calibration curve represents the relationship between the concentration of standard solutions and their absorbance at a specific wavelength, usually the maximum absorbance wavelength (λ max). In this study, a calibration curve was established using standard solutions with concentrations of 10, 20, 30, and 40 ppm. These specific concentrations were chosen to ensure accuracy of the measurements. Higher concentrations were excluded from the calibration curve because of their tendency to introduce errors into the results.

2.4.2 Effect of the concentration of adsorbate

After the λ max was determined, 50 mL from 10, 30, 50, and 70 ppm solutions were transferred to four urine cups by using a graduated cylinder, followed by the addition of 0.5 g of modified kaolinite, which was weighed carefully for each cup at a pH of 2. All the cups were then tightly closed and shaken at 200 rpm and 25 °C for half an hour. Each 5-minute portion from each cup was removed, the contaminated modified kaolinite was separated by centrifugation at 4000 rpm for 6 minutes, and the treated solution was analyzed via UV–Vis.

2.4.3 Effect of the amount of adsorbent

First**,** 0.1, 0.2, 0.3, 0.4, 0.5, and 0.6 g of modified kaolinite were weighed and transferred into six urine cups. Subsequently, 50 mL of 50 ppm solution was added via a graduated cylinder at a pH of 2, after which the cups were closed and shaken at 200 rpm and 25 °C for half an hour. Every 5 min, a portion from each sample was taken and then analyzed via UV–Vis at λ max = 464 nanometers.

2.4.4 Effect of pH

In this experiment, the effect of changing the pH was evaluated by varying the pH from 2 to 11. Each sample was prepared by weighing 0.5 g of modified kaolinite and placing it inside a urine cup, followed by the addition of 50 ml of 50 ppm solution. The pH was subsequently adjusted by using diluted solutions of HCl and NaOH. The samples were subsequently closed and shaken for half an hour at 200 rpm and 25 °C. A 5-minute portion of each sample was removed, after which the supernatant was analyzed.

2.4.5 Effect of temperature

To study the effects of changes in temperature, the process was carried out at four different temperatures: 17.5, 25, 32.5, and 40 °C. To prepare the samples, 0.5 g of modified kaolinite was placed in four urine cups, and then 50 mL of 60 ppm solution was added to each cup. The cups were subsequently tightly closed, and every cup was shaken at 200 rpm and a specific temperature for half an hour. Each 5-minute portion from each sample was taken, after which the solution was analyzed.

2.4.6 Recovery and reuse

2.4.6.1 Determination of the optimal thermolysis temperature

To determine the optimal temperature for reusing the material, a portion of MO was analyzed via thermogravimetric analysis (TGA) over a period of two hours. This analysis aimed to identify the temperature at which the MO underwent complete decomposition. The sample was heated gradually, and weight loss was monitored.

2.4.6.2 Decomposition of the sample

After the adsorption process was completed. The contaminated modified kaolinite was collected. The sample was placed in a crucible and subjected to thermal decomposition at 600 °C for one hour. After decomposition, the modified kaolinite was allowed to cool to room temperature.

Once the sample was prepared and the optimal thermolysis temperature determined, the first cycle was carried out with careful precision. First, 0.5 g of pretreated modified kaolinite, which had been heated up to 600 °C, was weighed. This was followed by the addition of 50 mL of a 50 ppm solution. The mixture was then shaken for half an hour at a speed of 200 rpm and a temperature of 25 °C at a pH of 2. After shaking, the contaminated kaolinite was collected for further treatment. The collected kaolinite underwent thermal decomposition at 600 °C for one hour. The previous step was meticulously repeated for each subsequent cycle to maintain consistency and accuracy in the experimental procedure.

2.5 Characterization

2.5.1 FT-IR

2.5.1.1 Phenazopyridine

Four distinct samples of pure modified kaolinite, pure PhPy, contaminated modified kaolinite, and modified kaolinite treated at 600 °C were characterized via Fourier transform infrared spectroscopy (FT-IR). This characterization was essential for demonstrating the processes of adsorption and thermal decomposition occurring within these materials.

2.5.1.2 Methyl orange

Three distinct samples, pure MO, contaminated kaolinite, and kaolinite treated at 600 °C, were characterized via Fourier transform infrared spectroscopy (FT-IR).

2.5.2 XRD and SEM

A sample of modified kaolinite was analyzed via X-ray diffraction (XRD), scanning electron microscopy (SEM). XRD analysis was conducted to determine the crystalline structure of the kaolinite samples. These peaks are essential for identifying the mineralogical composition and confirming the crystalline nature of kaolinite (84). In addition to XRD, SEM was employed to provide a visual representation of the microstructure of kaolinite. The SEM images captured the surface morphology and provided insights into the texture and particle size of the kaolinite samples. The high-resolution SEM images allowed examination of the shape and arrangement of the modified kaolinite particles. (84) Overall, the combination of XRD and SEM techniques provided a comprehensive understanding of the structural and morphological characteristics of the modified kaolinite sample (84).

Chapter Three
Results and Discussions

The results of studies of different parameters, including different concentrations of adsorbate, solution pH values, different amounts of adsorbent and temperatures, are disputed. All the data acquired from the UV- spectrophotometer and other instruments were plotted via Origin Pro 2024 software. Studying the adsorption isotherms, kinetics, and estimating the activation energy of the adsorption process helps elucidate the mechanism and nature of the interaction between the adsorbent and adsorbate. X-ray diffraction (XRD) and scanning electron microscopy (SEM) were used to determine the structural and morphological characteristics of the adsorbate.

In addition, FT-IR characterization was executed for the modified kaolinite before and after the adsorption process and after the thermal decomposition process to determine the changes on the surface of the composite and to determine the adsorption of the adsorbate on the adsorbent surface.

3.1 Comparison between kaolinite and modified kaolinite

The modification of kaolinite was executed to enhance the thermal stability. Many researchers documented that kaolinite is not a thermally stable at high temperatures, as Faqir et al. (85) showed in his research. Also, this was proven in Figure 3.1(a), which represented the TGA of kaolinite and modified kaolinite.

As seen in Figure 3.1 (b) and (c) that the modification of kaolinite did not affect it is adsorption capacity significantly, the adsorption efficiency of kaolinite at different concentrations is (88.65%, 85.43%, 79.78%, 67.55%) and (62.88% at 20, 30, 40, 60, and 80 ppm), respectively while the adsorption efficiency of modified kaolinite at different concentrations is (89%, 86%, 80%, 76%,) and (63% at 20, 30, 40, 60, and 80 ppm), respectively. On the other hand, the modification clearly enhances the thermal stability of kaolinite as seen in Figure 3.1 (a) and as documented by Wahyuni et al. in her research.

Figure 3.1

Comparison between kaolinite and modified kaolinite

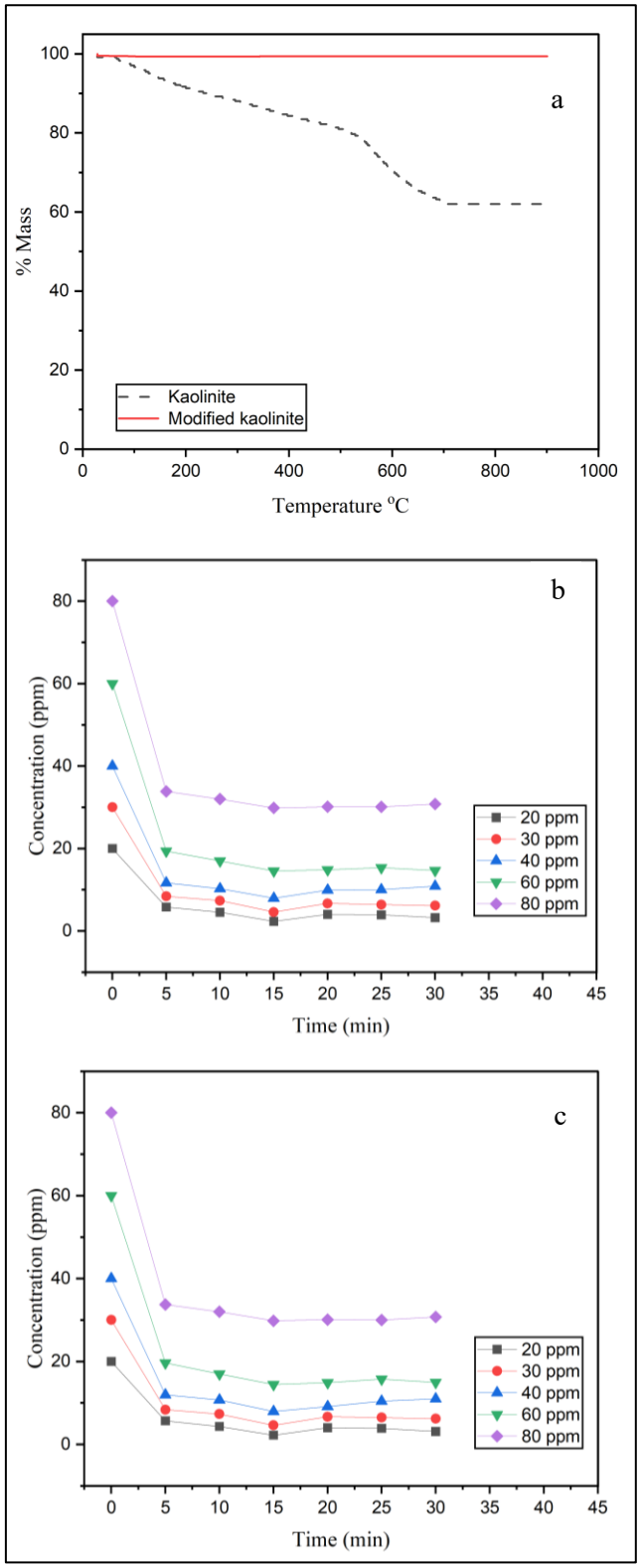

Note: (a) TGA results of kaolinite and modified kaolinite, (b) Adsorption of PhPy on kaolinite at various conditions: 0.5g/50mL, pH of 5, 200 rpm and 25 oC for half an hr (c) Adsorption of PhPy on modified kaolinite at various conditions: 0.5g/50mL, pH of 5, 200 rpm and 25 oC for half an *hr.*

3.2 Modified kaolinite characterization

3.2.1 XRD characterization

The X-ray diffraction (XRD) pattern of the modified kaolinite produced reflections corresponding to 275, 040, 183, 023, 046, 015, 09, 022, and 023 at angles of $12.^{1°}$, $20.^{28°}$, $24.^{68°}$, $35.^{78°}$, $38.^{28°}$, $45.^{38°}$, $50.^{82°}$, $55.^{14°}$, and $62.^{28°}$, respectively, as shown in Figure 3.2, and these numbers are consistent with the results reported by Tironi A et al. (86). The analysis was investigated using the Scherrer equation:

$$D = \frac{K\lambda}{\beta \cos\theta} \tag{7}$$

Where D is crystallite size in nm, K is the shape factor commonly equal 0.9, λ is wavelength of the X-ray source, β is the full width at half maximum (FWHM) of the diffraction peak in (radians), and Θ is Bragg angle in (radians).

To calculate the average particle size based on the width of the main diffraction peaks. The calculations donated an average particle size of approximately 15 nm. This fine particle size is indicative of the high surface area of modified kaolinite, which is crucial for its effectiveness as an adsorbent.

Figure 3.2

XRD pattern of modified kaolinite

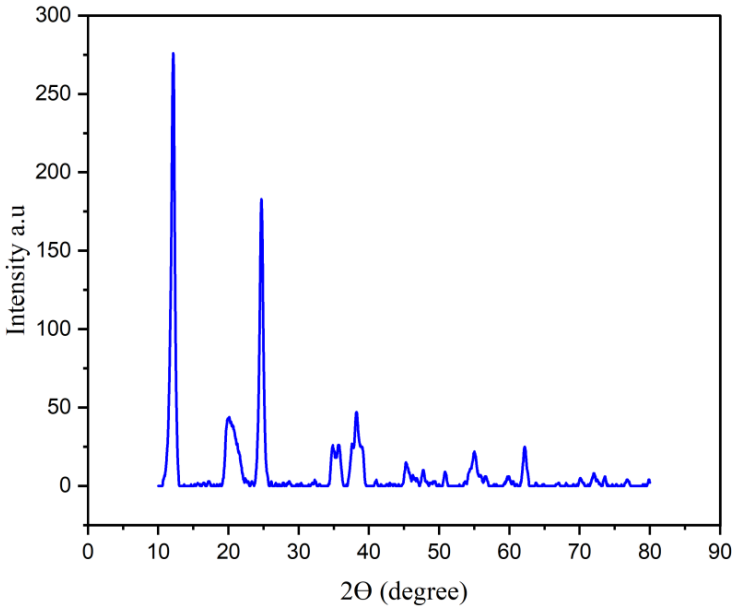

3.2.2 SEM characterization

The SEM image showed the presence of multilayered flakes formalized by agglomerated modified kaolinite nanoparticles. These flakes present an average size in the range of 5-10 µm as seen in Figure 3.3. The distinct layering observed in the SEM image is characteristic of modified kaolinite's structure, highlighting its platelet-like morphology. This layered structure contributes to the high surface area and adsorption capacity of modified kaolinite, promoting its effectiveness as an adsorbent material. The images also show a relatively uniform distribution of particle sizes, indicating consistency in the modified kaolinite powder preparation. These structural features, as visualized through SEM, are crucial for understanding the interaction of modified kaolinite with contaminants and its performance in adsorption applications.

Figure 3.3

SEM image of modified kaolinite

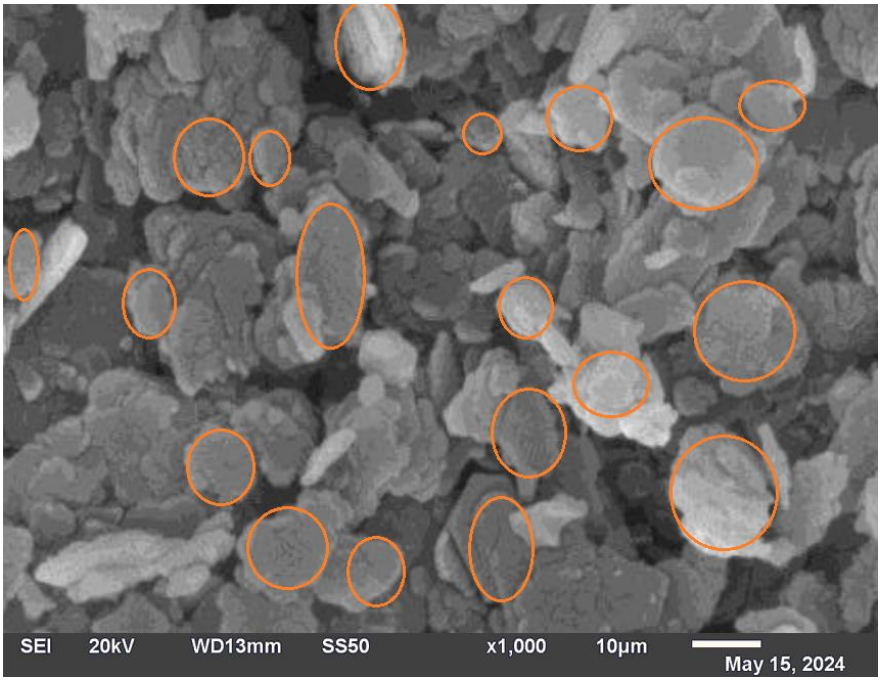

3.2.3 The point of zero charge pH (pzc)

During the adsorption process, the pH is a crucial factor that affects the adsorption capacity, and the surface charge of the adsorbent is determined by the surface zero-point charge (pH_{zcp}) (81). This has a considerable effect on the adsorption capacity. The pH_{zcp} of modified kaolinite was found to be 4.8, as shown in Figure 3.4. At this pH, the surface charge is zero but lower than 4.8, the surface charge is positive; on the other hand, when the pH is greater than 4.8, the surface charge is negative.

Figure 3.4

Plot of Δ (pH) vs. initial pH for modified kaolinite. The intercept shows the value of pH(zcp) for the solid. The results were obtained at room temperature

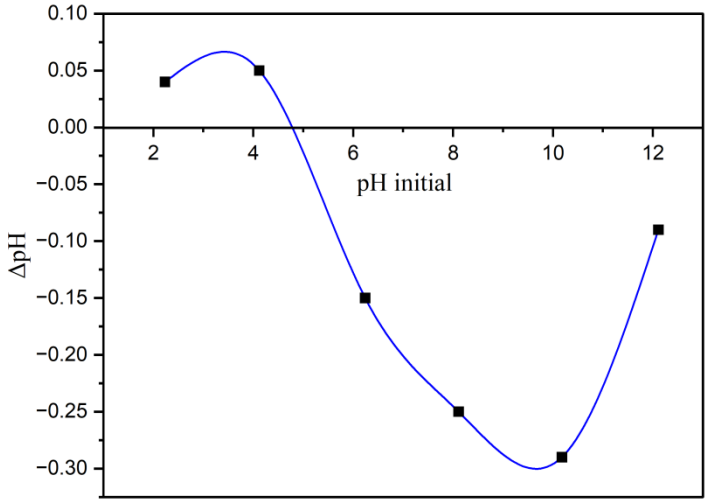

3.3 Phenazopyridine

3.3.1 Formation of the calibration curve

A calibration curve is an essential method to determine the concentration of an unknown sample in a solution by matching it to a series of standard solutions with their concentrations, which is related to the concentration of the prepared solution and its absorbance at λ max (82). Figure 3.5 shows a calibration curve of 5, 10, 20, 30, and 40 ppm solutions at λ max = 425 nm.

Figure 3.5

Calibration curve of PhPy

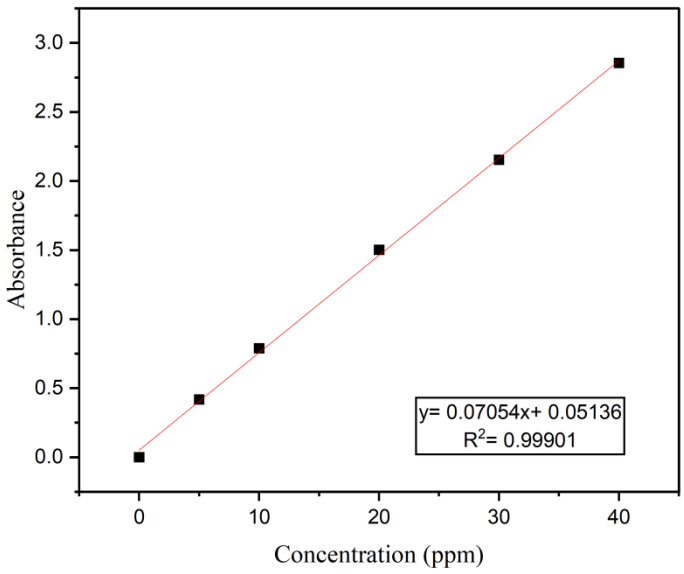

A linear equation is usually obtained for calibration curves. The correlation coefficient (R^2), which has the best fit when $R^2 = 1$, is usually utilized to determine the linearity of the calibration curve. The unknown concentration of the treated solutions was calculated via an equation obtained from the calibration curve.

3.3.2 Effect of the concentration of adsorbate

Studying the variation in the concentration of PhPy with the same amount of modified kaolinite is crucial for determining the saturation point of modified kaolinite where no more adsorption can occur since all available sites on the modified kaolinite are occupied by PhPy molecules. In addition, to construct adsorption isotherms, the adsorption efficiency of modified kaolinite, which varies with different concentrations, was determined.

As shown in Figure 3.6, the adsorption efficiency of modified kaolinite decreases as the concentration of PhPy increases. The adsorption efficiency at different concentrations is (89%, 86%, 80%, 76%) and (63% at 20, 30, 40, 60, and 80 ppm), respectively. These results indicate that modified kaolinite has a commendable adsorption efficiency. Even at high concentrations, it did not clearly decrease. It decreased from 87% to 63% for 20 ppm to 80 ppm.

Figure 3.6

Amounts of PhPy removed (ppm) over time under various conditions: 0.5 g/50 ml, 25 °C, 200 rpm, and pH = 5 for half an hr

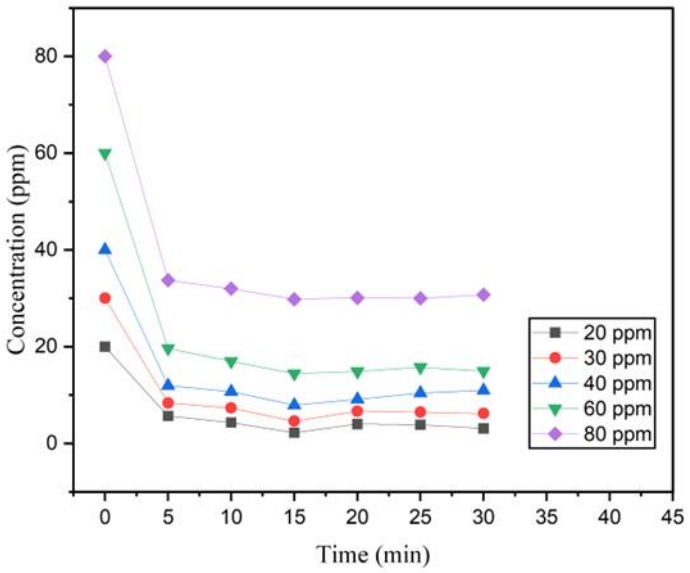

3.3.3 Effect of the amount of adsorbent

The amount of adsorbent affects the adsorption capacity of the modified kaolinite. This experiment aimed to determine the optimal quantity needed to achieve maximum adsorption and minimize waste.

In Figure 3.7. The effect of changing the amount of modified kaolinite from 0.1 to 0.6 g with PhPy concentrations of 30 and 60 ppm at a pH of 5 was shown. The percent removal of dye was calculated as follows:

$$\% \text{ of dye removal} = \frac{C_o - C_e}{C_o} \times 100 \quad (8)$$

where C_o and C_e (mg/L) are the initial and equilibrium concentrations of the dye in solution, respectively.

We noticed that the percent removal did not increase constantly with increasing amounts of modified kaolinite. As observed above at 30 ppm, an increase in the amount of modified kaolinite led to an increase in the percentage of dye removed to (74%) at 0.2 g. For 60 ppm, increasing the modified kaolinite amount led to an increase in the percentage of dye removed to (76%) at 0.5 g. Supplementally, increasing the modified kaolinite amount did not significantly affect the removal of dye. This is because the number of active adsorption sites on the adsorbent increases as the dosage of adsorbent increases.

However, increasing the dosage of modified kaolinite to more than 0.2 g for 30 ppm did not significantly increase the percent removal. For 60 ppm, increasing the amount of modified kaolinite to more than 0.5 g did not significantly increase the percent removal.

Figure 3.7

Effect of adsorbent amount (g) on the removal efficiency of the PhPy

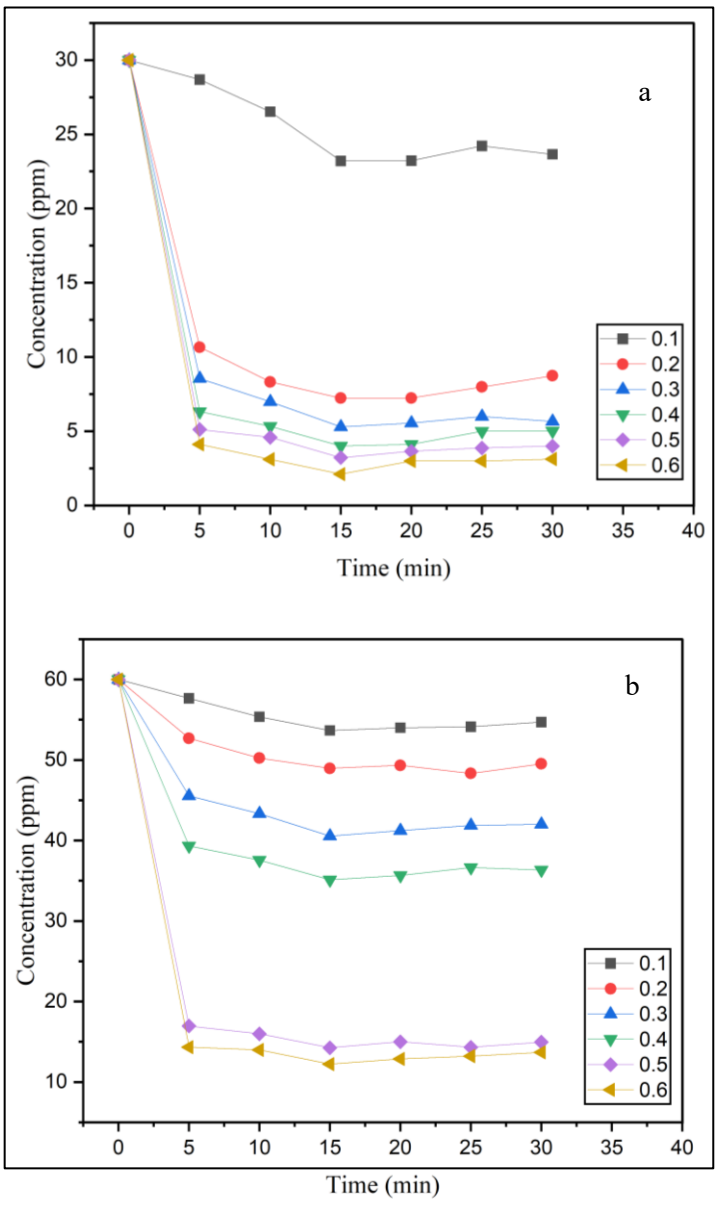

Note: (a) At 30 ppm and (b) 60 ppm, the solution volume was 50 mL, the pH was 5, the mixture was shaken at 200 rpm for half an hour at 25 °C.

3.3.4 Effect of pH

The adsorption of two different concentrations of PhPy, high at 60 ppm and low at 30 ppm, on modified kaolinite was examined across a pH range of 3--11. Each experiment utilized 0.5 g with 50 mL for 60 ppm and 0.2 g with 50 mL for 30 ppm, and the mixture was continuously shaken for 60 minutes. The adsorption efficiency was affected by pH and the surface charge of the modified kaolinite, represented by $pH_{(zcp)}$. The equilibrium PhPy structure at a given pH clarifies how the surface charge of modified kaolinite and PhPy changes with varying pH. The adsorption results at different pH values are shown in Figure 3.8.

Figure 3.8

Effects of pH on the removal efficiency of PhPy

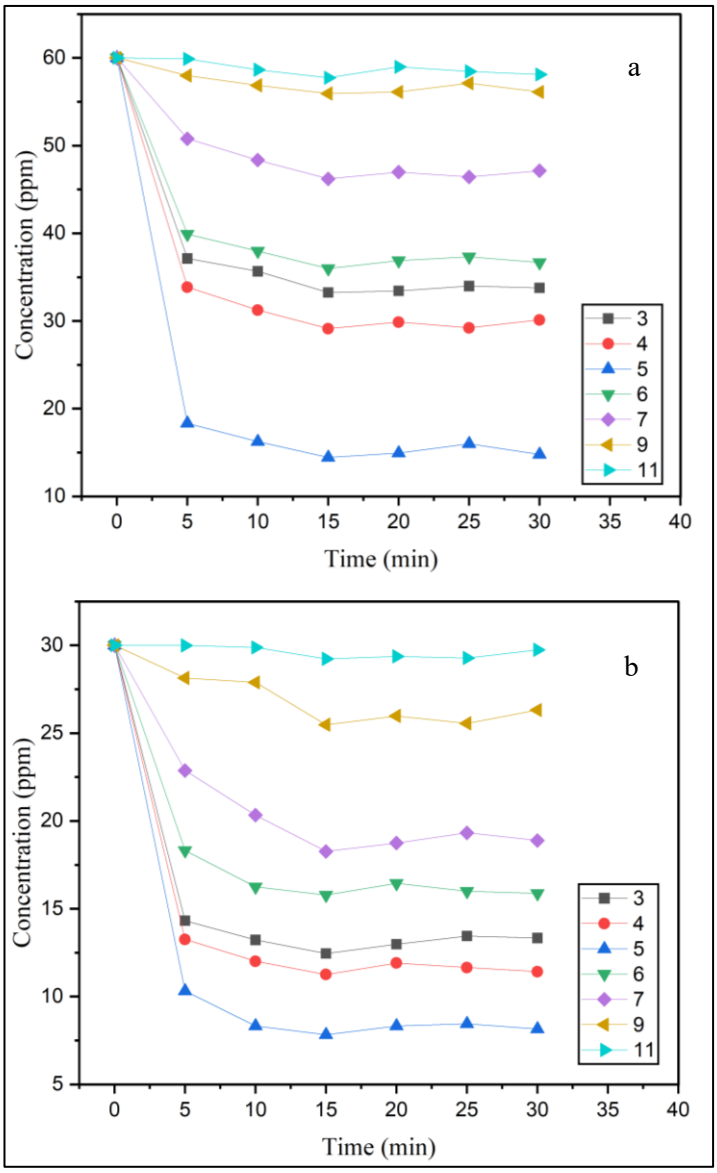

Note: (a) 0.2 g/30 ppm and (b) 0.5 g/60 ppm at 200 rpm for half an hour at 25 °C.

The results showed that the ideal pH for the adsorption of PhPy for 30 and 60 ppm was 5. The percent removal reached 74% for 30 ppm and 76% for 60 ppm. At a pH of 5, the surface charge of modified kaolinite was negative, whereas that of PhPy was positive, so electrostatic attraction occurred. At pH values of 3 and 4, the surface charge of the modified kaolinite was positive, and the PhPy had positive ions. This limits electrostatic attraction. At a pH of 6, the surface charge of modified kaolinite was negative, whereas the surface charge of PhPy was neutral to positive ions, which limits electrostatic attraction and repulsion. At pH 7, the surface charge for the composite was negative, and that for PhPy was neutral, which led to a decrease in electrostatic attraction. For pH values of 9 and 11, the surface charge of the clay was negative, as was the case for PhPy, which has negative species, and repulsion occurred, which led to a decrease in the percent removal. However, the order of adsorption of PhPy on modified kaolinite from the most to the least efficient is $5 > 4 > 3 > 6 > 7 > 9 > 11$.

3.3.5 Adsorption Isotherms

Adsorption isotherms clarify adsorption processes and capacity. The most common adsorption isotherms are the Langmuir and Freundlich isotherms.

The equilibrium adsorption isotherms of PhPy on modified kaolinite were obtained using initial PhPy concentrations of 20, 30, 40, 60, and 80 ppm at 25 °C, a pH of 5, and a shaking time of half an hour. The solid/solution ratio was 0.5 g/50 mL. The results were represented by Langmuir and Freundlich isotherm models to perform PhPy adsorption on the adsorbent and equilibrium concentration. The adsorption isotherms of PhPy on modified kaolinite are represented in Figure 3.9 (a). The plots of C_e versus q_e for the adsorption isotherms, C_e/q_e versus C_e for the Langmuir equation are represented in Figure 3.9 (b), and $log\ q_e$ versus $log\ C_e$ for the Freundlich isotherm are shown in Figure 3.9 (c).

Figure 3.9

(a) Adsorption isotherms of PhPy onto modified kaolinite, (b) Langmuir isotherm, and (c) Freundlich isotherm

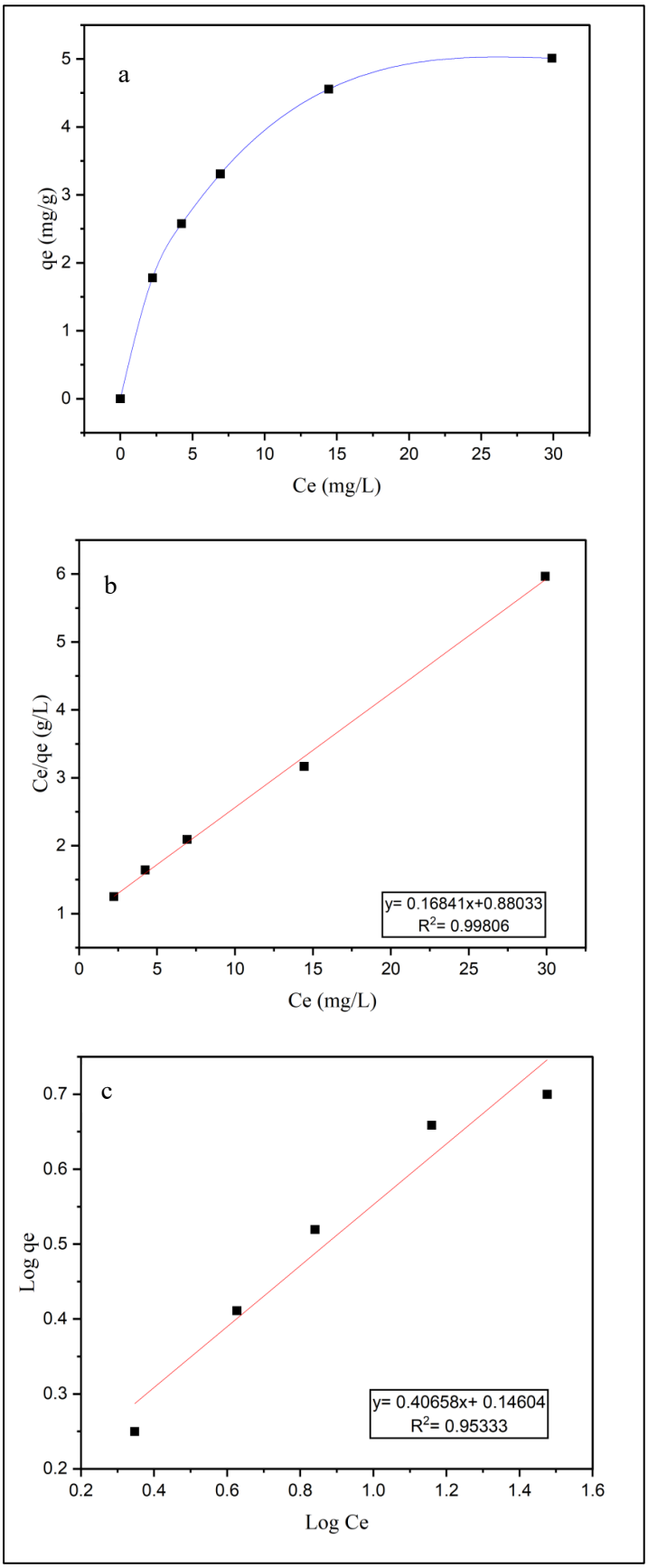

The slope and intercept were recorded from the equations that extracted from these graphs and were used to determine the Langmuir and Freundlich isotherm parameters. The resulting values and correlation coefficients for PhPy adsorption on modified kaolinite are presented in Table 3.1.

Table 3.1

Langmuir and Freundlich isotherm parameters and correlation coefficients for PhPy adsorption onto modified kaolinite

Langmuir			Freundlich		
Q_o (mg/g)	b (L/mg)	R^2	K_f ((mg/g) (L/mg)$^{1/n}$))	1/n	R^2
5.9378	0.1913	0.99806	1.3997	0.40658	0.95333

As shown in Table 3.1, the adsorption of PhPy was completely adapted with the Langmuir isotherm model, with a higher R^2 equal to 0.99806. This confirmed that the adsorption occurred at specified homogenous sites inward from the adsorbent, formalizing a single layer covering the surface of the adsorbent. In addition, the Freundlich constant 1/n was found to equal 0.40658. This indicated that the Langmuir isotherm is more favorable. Generally, the results confirmed that the adsorption process in this study obeys the Langmuir isotherm model.

3.3.6 Adsorption kinetics

Studying the kinetics of adsorption is important. The adsorption rate must be studied to realize a kinetic model that represents the adsorption process. The kinetics of adsorption determine the rate at which the adsorbate interacts with the adsorbent and the time ordered to obtain adsorption completion (87).

Some of the commonly used kinetic models include the pseudo first- and second-order rate models, the Adam–Bohart–Thomas relation, the intraparticle diffusion model, Weber and Morris sorption, the first-order equation of Bhattacharya and Venkobachar, the external mass transfer model, and the first-order reversible reaction model (87).

In this study, three kinetic models for PhPy adsorption on modified kaolinite were executed: the pseudo-first-order model, the pseudo-second-order model, and the intraparticle diffusion model, which are represented by these three equations (88).

$$\log (q_e - q_t) = \log q_e - \frac{k_1}{2.303} t \quad (9)$$

where q_e and q_t (mg/g) are the masses of adsorbate per unit mass of adsorbent at equilibrium and at time t (min), respectively, and where k_1 (min^{-1}) is the rate constant of the pseudo-first-order model (88).

$$\frac{t}{q_t} = \frac{1}{k_2 q_e^2} + \frac{1}{q_e} t \quad (10)$$

where q_e and q_t (mg/g) are the masses of adsorbate per unit mass of adsorbent at equilibrium and at time t (min), respectively. k_2 (g/mg min) is the pseudo-second-order rate constant of adsorption. (89)

$$q_t = k_p t^{0.5} + b \quad (11)$$

where q_t (mg/g) is the mass of adsorbate per unit mass of adsorbent at time t (min), k_p (mg/g $min^{0.5}$) is the rate constant of intraparticle diffusion and b is a constant that indicates the thickness of the boundary layer.

This experiment was investigated by using a 0.5 g/50 mL 60 ppm solution of PhPy. At a pH of 5, the mixture was shaken at 200 rpm and 25 °C for half an hour. The data were then plotted for pseudo-first-order Log(qe-qt) vs. t, as shown in Figure 3.10 (a), while for pseudo-second-order, t/qt vs. t was plotted, as represented in Figure 3.10 (b), and for intraparticle diffusion, qt vs. $t^{0.5}$ was plotted, as shown in Figure 3.10 (c).

Figure 3.10

(a) Pseudo first-order, (b) Pseudo second-order, and (c) Intra particle diffusion

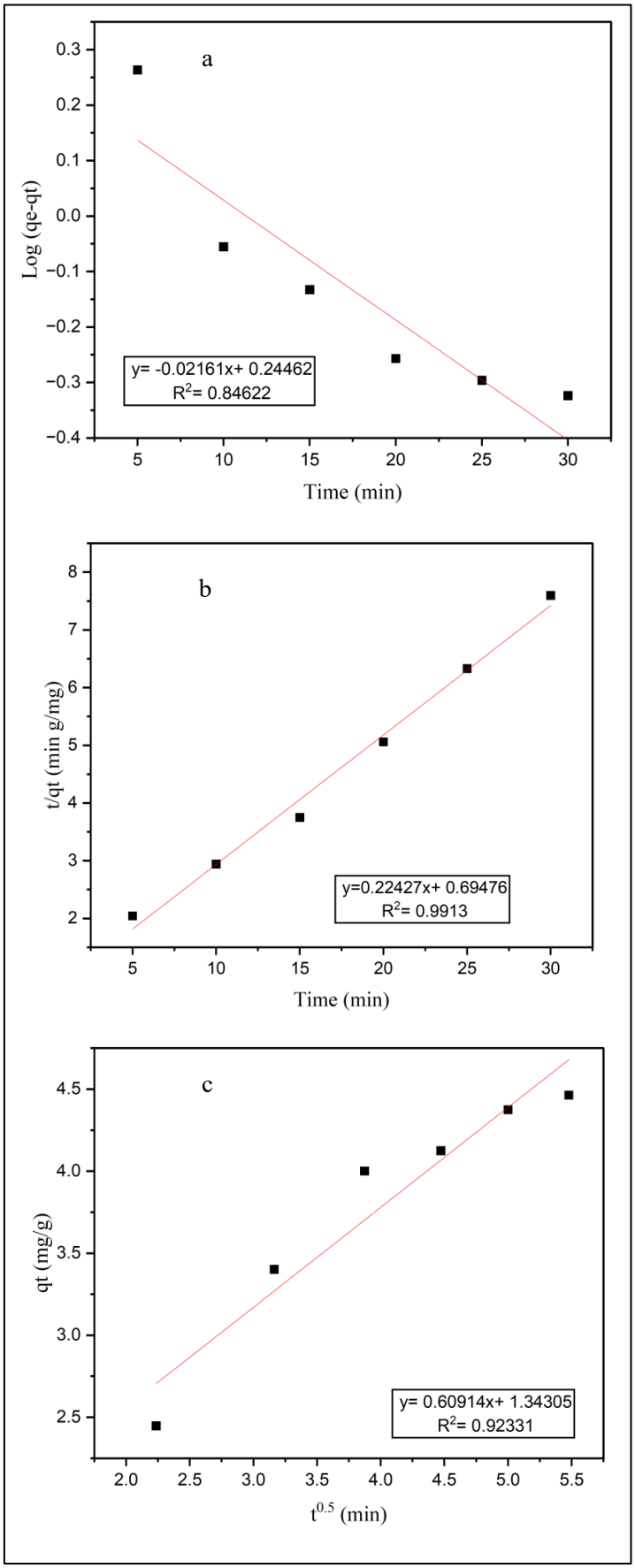

Table 3.2 shows the correlation coefficients and parameters for the pseudo second-order, pseudo first-order, and intraparticle diffusion models. These results indicate that the pseudo second-order model is more appropriate for depicting the adsorption mechanisms on the adsorbent. The R^2 values are closer to 1 in the pseudo second-order model. On the other hand, the correlation coefficients are lower in the pseudo-first-order model. The calculated q_e values for the adsorbent closely stratify with the experimental values, confirming the appropriateness of the pseudo second-order model. In addition, the intraparticle diffusion model highlights that the rate is confined by mass transfer toward the boundary layer, which is evident from the non-origin passing straight line with correlation coefficients.

Table 3.2

Pseudo first-order and pseudo second-order kinetic models and intra particle diffusion kinetic model parameters and correlation coefficients for PhPy adsorption onto modified kaolinite

Pseudo first-order			
q_e (Exp) (mg/g)	K_1(min^{-1})	q_e(calc.) (mg/g)	R^2
4.22316	0.5634	1.7563	0.84622
Pseudo second-order			
	K_2 (g/mg min)	q_e(calc.) (mg/g)	R^2
	0.0758	4.4589	0.9913
Intra particle diffusion			
	K_p (mg/g $min^{1/2}$)	b	R^2
	0.60914	1.34305	0.92331

3.3.7 Effect of temperature

Studying the effect of temperature on the adsorption process is an essential step (90). Understanding the mechanism of the adsorption process is important. In addition, activation energy has been investigated (91). Hence, Worthy information about the nature of process and mechanism was obtained by studying the effects of temperature (92).

The equilibrium adsorption capacity of an adsorbent may be affected by varying the temperature. For example, the adsorption capacity decreases when the temperature increases for an exothermic reaction; however, it evolves into an endothermic reaction (93).

In this study, the adsorption of PhPy on modified kaolinite was studied at temperatures of 17.5, 25, 32.5, and 40 °C at 30 and 60 ppm, and the results are shown in (Appendix A1).

As shown in (Appendix A1), the adsorption capacity decreases as the temperature increases. This decrease in PhPy removal suggests that the adsorption of PhPy on the modified kaolinite surface is an exothermic process. According to different studies, such as that of Alkan et al. (93), when adsorption decreases while the temperature increases, this is due to the softened adsorptive forces between the adsorbate species and the active sites of the adsorbent. Therefore, when the temperature increases, the desorption process prevails because of the soft interaction in the adsorption system.

3.3.8 Determination of the activation energy

The experimental data collected at different temperatures from (Appendix A1 (b)) in the previous section were used to resolve the activation energy, via Arrhenius equation. In general, finding the activation energy provides beneficial information about the type of process and adsorption mechanism.

The Arrhenius equation was represented in the following formula: (92)

$$k = Ae^{-Ea/RT} \tag{12}$$

Arrhenius equation could be converted to the linear form as in the following equation:

$$ln\, k = \frac{-Ea}{RT} + lnA \tag{13}$$

where T is the temperature in Kelvin, R is the ideal gas constant (R= 8.314 J/mol K), k is the rate constant, and A is Arrhenius constant. k can be expressed as $(C_t - C_o)/t$ in (sec), where C_o and C_t (mg/L) represent the initial and equilibrium adsorbate concentrations, t represents time.

The values of Ea and Arrhenius constant can be determined by plotting 1/T vs Ln k, as presented in (Appendix A2). From the slope and intercept in (Appendix A2), Ea and Arrhenius constant were calculated via Eq. (13). The calculation of activation energy at the studied temperatures are presented in Table 3.3

Table 3.3

The calculations of activation energy for the adsorption of PhPy onto modified kaolinite at different temperatures

Ea (KJ/mol)	Ln A	R^2
27.2601	13.305	0.9987

As shown in Table 3.3, the value of Ea provides information about the adsorption system, which can be used to understand the mechanism and nature of the adsorption process. The previous studies explored the determination of the Ea value, which is related to the nature of the adsorption process. Aljamali et al. (94) reported that when Ea is less than 40 kJ/mol, the adsorption process corresponds to physical process. Hence, the Ea was found to be 27.2601 KJ/mol, indicating that the adsorption process between modified kaolinite and PhPy follows the physical adsorption process.

3.3.9 Recovery and reuse

3.3.9.1 TGA characterization

Before recovering the contaminated modified kaolinite, the thermal stability of modified kaolinite was examined via TGA. The observation of a straight line indicates that modified kaolinite is stable at very high temperatures with time. Additionally, the PhPy was analyzed via TGA. To determine the optimal temperature for treatment. At this temperature, the PhPy should decompose completely. (Appendix A3) shows the TGA results of the PhPy and modified kaolinite.

As shown in (Appendix A3), the modified kaolinite was thermally stable since it formed a straight line at very high temperatures with time. While PhPy has thermal stability up to 200 °C, it decomposes at 3 different stages. The first stage is from 200 to 300 °C. PhPy lost 30% of its components, associated with NH_3 and CH_4 gases. The second stage from 300 to 400 °C resulted in the loss of another 30% due to the loss of the azo group, which was proposed to break. The final stage from 400 to 600 °C PhPy lost the last 40%, which was suggested to be the bulk organic group, such as the benzene ring.

3.3.9.2 Reuse cycles

After the optimal temperature was determined and the adsorption process was finished, the contaminated modified kaolinite was regenerated and calcined at 600 °C for one hour. This led to complete decomposition of the adsorbed PhPy.

(Appendix A4) shows that the annealed composite can be reused multiple times without any significant effect on the removal efficiency, where the percent removal of PhPy for 4 cycles ranged between (71%) and (75%) for 60 ppm, comparing these results with percent removal of fresh modified kaolinite which equal 75%, this indicating that the thermal stability of modified kaolinite will have a massive effect when it is related to reuse for future adsorption techniques for water organic pollution.

The thermal decomposition of PhPy, which is adsorbed on modified kaolinite and reused multiple times, is an effective method from an environmental and economic standpoint. This minimizes waste generation and the requirement of persistent replacement of adsorbents. This makes the process environmentally friendly and cost-effective.

3.3.10 FT-IR characterization

To confirm the adsorption process of PhPy at the modified kaolinite surface, the samples of PhPy, modified kaolinite, PhPy on modified kaolinite and PhPy onto modified kaolinite after thermal decomposition at 600 °C were characterized via FT-IR, as shown in (Appendix A5 (a)). The modified kaolinite has adsorption bands between 3619 and 3689 cm^{-1} for the OH stretching group, where the bands at 1004, 1028, and 1113 cm^{-1} correspond to Si–O stretching, the peak at 911 cm^{-1} corresponds to Al–OH stretching, and the remaining peaks correspond to Si–O–Al stretching (86).

In (Appendix A5 (b)), PhPy has peaks at 3335 and 3290 $cm^{-1,}$ which indicate N–H stretching for the primary amine; at 3065 and 2908 cm^{-1}, C–H stretching occurs; at 1635 cm^{-1}, N–H bending occurs; at 1601 cm-1, C=N stretching occurs; and at 1449 cm^{-1}, N–N=N; at 1267 $cm^{-1,}$ C–N for the aromatic amin (95).

In (Appendix A5 (c)), PhPy peaks in the range of 1200–3400 cm^{-1} were observed, which indicated that PhPy was adsorbed onto the modified kaolinite surface. As shown in (Appendix A5 (d)), after thermal decomposition, all the peaks of PhPy disappeared, but the peaks of modified kaolinite remained the same. This proves that thermal

decomposition resulted in the complete removal of PhPy from the surface of the composite.

3.4 Methyl orange

3.4.1 Formation of the calibration curve

A calibration curve is an essential method to determine the concentration of an unknown sample in solution by matching it to a series of standard solutions with their concentrations, as mentioned in section 3.3.1. (Appendix A6) shows a calibration curve of 10, 20, 30, and 40 ppm solutions at λ max = 464 nm.

The correlation coefficient (R^2), which is equal to 0.99961, indicates that the calibration curve has ideal linearity. The equation derived from the curve was used to determine the concentration of unknown samples.

3.4.2 Effect of the concentration of adsorbate

The variation in the concentration of MO when a fixed amount of modified kaolinite is used is crucial for constructing adsorption isotherms and determining the saturation point of modified kaolinite, where no more adsorption can occur. Additionally, the adsorption efficiency of modified kaolinite, which varies with different concentrations, was determined.

As shown in (Appendix A7), the adsorption efficiency of the modified kaolinite decreases when the concentration of MO increases. The adsorption efficiency at different concentrations was 89%, 85%, 74%, and 66% at 10, 30, 50, and 70 ppm, respectively. These results indicate that modified kaolinite has a noteworthy adsorption efficiency.

3.4.3 Effect of the amount of adsorbent

The effects of varying the amount of adsorbent on the adsorption capacity of the adsorbent were studied. This experiment aimed to determine the optimal quantity needed to achieve maximum adsorption and minimize waste.

(Appendix A8) shows the impact of changing the amount of modified kaolinite from 0.1 to 0.6 g while fixing the concentration of the dye to 50 ppm at a pH of 2. The percent removal of the dye was calculated as follows:

$$\% \text{ of dye removal} = \frac{C_o - C_e}{C_o} \times 100 \quad (14)$$

where C_o and C_e (mg/L) are the initial and equilibrium concentrations of the dye in solution, respectively.

We noticed that the percent removal did not increase constantly with increasing amounts of modified kaolinite. As seen above, at 50 ppm, the increase in the modified kaolinite amount led to an increase in the percentage of dye removed to 74% for 0.5 g. Supplementally, increasing the modified kaolinite amount did not significantly affect the removal of dye. This is because the number of active adsorption sites on the adsorbent increases as the dosage of adsorbent increases. However, increasing the dosage of modified kaolinite to more than 0.5 g at 50 ppm did not significantly increase the percent removal.

3.4.4 Effect of pH

The adsorption of MO at 50 ppm on modified kaolinite was tested across a pH range of 3--11. The mixture was continuously shaken for 30 minutes. The adsorption efficiency was affected by pH and the surface charge of the modified kaolinite, represented by pH_{zcp}. The equilibrium MO structure at a given pH clarifies how the surface charge of modified kaolinite and MO changes with varying pH. The adsorption results at different pH values are shown in (Appendix A9).

As shown in (Appendix A9), the optimal pH for the adsorption of MO at 50 ppm was 2, where the percentage removal reached 74% at 50 ppm. At a pH of 2, the surface charge of modified kaolinite was positive, whereas MO had slightly negative ions, so electrostatic attraction occurred. At pH values of 4 and 5, the surface charge of the modified kaolinite was positive, and the MO had neutral to positive ions, which limited electrostatic attraction. At a pH of 7, the surface charge of the composite was negative, whereas that of MO was neutral, which led to a decrease in electrostatic attraction. At pH values of 9 and 11, the surface charge of the clay was negative, as was the case for MO, which has negative species, and repulsion occurred, which led to a decrease in the percentage of removal. However, the order for the adsorption of MO onto modified kaolinite from the most to the least efficient is $2 > 4 > 5 > 7 > 9 > 11$.

3.4.5 Adsorption Isotherms

Adsorption isotherms clarify adsorption processes and capacity. The most common adsorption isotherms are the Langmuir and Freundlich isotherms, and the equations are presented in section 3.3.5.

The equilibrium adsorption isotherms of MO on modified kaolinite were executed using initial MO concentrations of 10, 30, 50, and 70 ppm at 25 °C, a pH of 2, a shaking time of 30 min, and a solid/solution ratio of 0.5 g/50 mL. The results were plotted via the Langmuir and Freundlich isotherm models to describe MO adsorption on the adsorbent and the equilibrium concentration. The plot of the adsorption isotherms of MO adsorption on modified kaolinite is presented in (Appendix A10 (a)). The plots of C_e versus q_e for the adsorption isotherms, C_e/q_e versus C_e for the Langmuir equation are represented in (Appendix A10 (b)), and *log* q_e versus *log* C_e for the Freundlich isotherm are shown in (Appendix A10 (c)).

The slope and intercept were taken from the equations obtained from these graphs and were used to determine the Langmuir and Freundlich isotherm parameters. The resulting values and correlation coefficients for MO adsorption on modified kaolinite are presented in Table 3.4.

Table 3.4

Langmuir and Freundlich isotherm parameters and correlation coefficients for MO adsorption onto modified kaolinite

Langmuir			Freundlich		
Q_o (mg/g)	b (L/mg)	R^2	K_f ((mg/g) (L/mg)$^{1/n}$))	1/n	R^2
2.4137	0.6472	0.9987	0.9618	0.4274	0.9524

As shown in Table 3.4, the adsorption of MO was completely adapted with the Langmuir isotherm model, with a high R^2 equal to 0.9987. This confirmed that the adsorption occurred at specified homogenous sites inward from the adsorbent, formalizing a single layer covering the surface of the adsorbent. In addition, the Freundlich constant 1/n was found to be 0.4274. This indicated that the Langmuir isotherm is more favorable. Generally, the results confirmed that the adsorption process in this study obeys the Langmuir isotherm model.

3.4.6 Adsorption kinetics

In this study, three kinetic models for MO adsorption on modified kaolinite were executed: the pseudo-first-order model, the pseudo-second-order model, and the intra particle diffusion model. These equations are presented in section 3.3.6.

This experiment was investigated by using 0.5 g/50 mL of a 50ppm solution of MO under the following conditions: pH of 2, shaking speed of 200 rpm, and 25 °C for half an hour. The data were then plotted for the pseudo-first-order Log(qe-qt) vs t, as represented in (Appendix A11 (a)). The pseudo-second-order t/qt vs t is represented in (Appendix A11 (b)), and the intraparticle diffusion qt vs $t^{0.5}$ is represented in (Appendix A11 (c)).

Table 3.5 shows the correlation coefficients and parameters for the second-order, pseudo-first-order, and intraparticle diffusion models. These results indicate that the pseudo-second-order model is more appropriate for depicting the adsorption mechanisms on the adsorbent. The R^2 values are closer to 1 in the pseudo second-order model. On the other hand, the correlation coefficients are lower in the pseudo-first-order model. The calculated q_e values for the adsorbent closely stratify with the experimental values, confirming the appropriateness of the pseudo-second-order model. In addition, the intraparticle diffusion model highlights that the rate is confined by mass transfer toward the boundary layer, which is evident from the non-origin passing straight line with correlation coefficients.

Table 3.5

Pseudo first-order and pseudo second-order kinetic models, and intraparticle diffusion kinetic model parameters and correlation coefficients for MO adsorption onto modified kaolinite

Pseudo first order			
q_e (Exp) (mg/g)	K_1(min^{-1})	q_e(calc.) (mg/g)	R^2
3.3333	-0.01143	1.3212	0.91043
Pseudo second order			
	K_2 (g/mg min)	q_e(calc.) (mg/g)	R^2
	0.1816	3.4913	0.9881
Intra particle diffusion			
	K_p (mg/g $min^{1/2}$)	b	R^2
	0.4054	1.5239	0.92861

3.4.7 Effect of temperature

The equilibrium adsorption capacity of the adsorbent may be affected by varying the temperature. For example, the adsorption capacity decreases when the temperature increases for an exothermic reaction; however, it evolves for an endothermic reaction, as mentioned in section 3.3.7.

In this study, the adsorption of MO on modified kaolinite was studied at temperatures of 17.5, 25, 32.5, and 40 °C at 50 ppm, and the results are shown in (Appendix A12).

As shown in (Appendix A12), the adsorption capacity decreases when the temperature increases. This decrease in MO removal suggests that the adsorption of MO on the modified kaolinite surface is an exothermic process. According to different studies, such as that of Alkan et al. (93), when adsorption decreases while the temperature increases, this is due to the softened adsorptive forces between the adsorbate species and the active sites of the adsorbent. Therefore, when the temperature increases, the desorption process prevails because of the soft interaction in the adsorption system.

3.4.8 Determination of the activation energy

The data obtained from (Appendix A12) in the previous section were resolved to determine the activation energy, as described in section 3.3.8

The values of Ea and Arrhenius constant can be determined by plotting 1/T vs Ln k, as presented in (Appendix A13). From the slope and intercept in (Appendix A13), Ea and Arrhenius constant were calculated via Eq. (13). The activation energy calculations at the studied temperatures are presented in Table 3.6.

Table 3.6

The calculations of activation energy for the adsorption of MO onto modified kaolinite at different temperatures

Ea (KJ/mol)	Ln A	R^2
39.2587	18.476	0.99912

As shown in Table 3.6, the Ea magnitude obtained in this study was 39.2587 kJ/mol. This value confirmed that the adsorption process obeyed physical adsorption which indicated the weak interaction between adsorbate and adsorbent surface, these interaction

represented by Van Der Waals forces, this because the value is lower than 40 KJ/mol as Aljamali et al. (94) documented in his research.

3.4.9 Recovery and reuse

3.4.9.1 TGA characterization

MO was analyzed via TGA to determine the optimal temperature for reuse. At this temperature, MO should decompose completely. (Appendix A14) shows the TGA results for MO and modified kaolinite.

As shown in (Appendix A14), the modified kaolinite was thermally stable, as a straight line was observed at very high temperatures with time. MO decomposed at 3 different stages. In the first stage from 100 to 250 °C, 30% of the MO is lost as components, which are proposed to be NH_3, CH_4, and SO_2 gases. During the second stage from 250 to 450 °C, MO lost another 30% of the total energy due to the loss of the azo group, which was proposed to break. The final stage from 450 to 600 °C MO resulted in the loss of the last 40%, which was suggested to be due to the bulk organic group, such as the benzene ring.

3.4.9.2 Reuse cycles

After the optimal temperature was determined and the adsorption process was finished, the contaminated modified kaolinite was regenerated and calcined at 600 °C for half an hour. This led to complete decomposition of the adsorbed MO.

In this experiment, 0.5 g of the treated modified kaolinite was mixed with 30 ppm kaolinite and shaken for half an hour at a pH of 2, 200 rpm and 25 °C. (Appendix A15) shows that the annealed composite can be reused multiple times without any significant impact on removal efficiency. The percentage of MO removed after 4 cycles ranged between 81% and 85% comparing these results with percent removal of fresh modified kaolinite which equal 68%, these findings indicate that the thermal stability of modified kaolinite has an enormous effect on reuse for future adsorption techniques for water organic pollution.

3.4.10 FT-IR characterization

To confirm the adsorption process of MO at the modified kaolinite surface, the samples of MO, modified kaolinite, MO on modified kaolinite and MO on modified kaolinite after thermal decomposition at 600 °C were characterized via FT-IR. As shown in (Appendix A16 (a)), the modified kaolinite has adsorption bands between 3619 and 3689 cm^{-1} for the OH stretching group. The bands at 1004, 1028, and 1113 cm^{-1} represent Si–O stretching. The peak at 911 cm^{-1} corresponds to Al-OH stretching. The remaining peaks indicate Si–O–Al stretching (86).

In (Appendix A16 (b)), MO has a peak at 1606 $cm^{-1,}$ which indicates C-C stretching for the benzene ring; 1368 cm^{-1} indicates N=N; 1193 $cm^{-1,}$ for C-N stretching; 1117 $cm^{-1,}$ for SO_3^- stretching; and 1038 and 1005 cm^{-1}, for SO stretching (96).

As shown in (Appendix A16 (c)), MO peaks in the range of 1000–1700 cm^{-1} were observed. This indicates that MO was adsorbed onto the modified kaolinite surface. As shown in (Appendix A16 (d)), after thermal decomposition, all the peaks of MO disappeared, but the peaks of modified kaolinite remained the same. This proves that thermal decomposition completely removed MO from the surface of the composite.

3.5 Conclusion

This study revealed that thermolysis decomposition could be used as a technique for the reuse of modified kaolinite, which is utilized to adsorb PhPy and MO. This is a new technique inserted into the world of reuse. The effects of various parameters were evaluated, and the results revealed that the adsorption process was dependent on the concentration of the dye, the amount of modified kaolinite, the temperature, the pH, and time. For both dyes, the percent removal increased when the amount of modified kaolinite and time increased and when the temperature decreased. Ultimate elimination was obtained at a pH of 5 for PhPy, which reached 76%, and for MO, which reached (74%), the pH was 2.

The Freundlich and Langmuir models were selected from different adsorption isotherm models and studied. The results confirmed that the adsorption process for both dyes obeyed the Langmuir isotherm. This result indicated that the adsorption occurred in a single layer and was homogenous. The results from studying three different kinetics models revealed that the adsorption of both dyes on modified kaolinite followed the

pseudo second-order rate model. Estimating the activation energy of the adsorption of the two dyes on the modified kaolinite confirmed that the process followed a physical adsorption process.

Physical processes reveal that there are soft interactions between modified kaolinite and both dyes. Additionally, the desorption process can occur. Therefore, the recovery studies were investigated via thermal decomposition, and the results emphasized that the modified kaolinite can be reused for four cycles. In conclusion, modified kaolinite is an effective and inexpensive adsorbent that is simple to reuse. All the results obtained in this study confirmed that the adsorption process using modified kaolinite is beneficial, simple, and cost-effective. Additionally, the efficiency of thermal decomposition, which is environmentally friendly, should be explored. This makes all processes, ranging from adsorption to thermal decomposition, adequate for mutating from batch experiments to large-scale industries.

3.6 Future work

Our future work should focus on converting batch experiments to continuous experiments by using columns for removing PhPy and MO dyes or other organic contaminants. After that, the column will be thermally decomposed at high temperature and then ready for use again.

Other methods can be applied, such as organic modification of kaolinite instead of the use of $ZnCl_2$. This could be achieved by adsorption at the surface of kaolinite by natural dyes such as anthocyanin or carotene. Then, the adsorption process was investigated to treat polluted water from organic contamination.

In addition, thermal decomposition can be applied to other types of clays and other types of organic contamination. Also, in thermal decomposition, various temperature below than 600 ^{o}C could be used to check if it suitable to completely decomposition of the dyes. In the thermal process, the clay can be modified by washing it with an acidic solution, basic solution or ionic solution.

List of Abbreviations

Abbreviation	Meaning
Ea	Activation Energy
K	Adsorption Equilibrium Constant
AOP	Advanced Oxidation Process
q_e	Amount of Adsorbate Per Unit of Adsorbent
A	Arrhenius Constant
C_t	Concentration of Adsorbate in the Solution at Time t
R^2	Correlation Coefficient
C_e	Equilibrium Concentration of Adsorbate in the Solution
FT-IR	Fourier Transform Infrared Spectroscopy
K_f	Freundlich Isotherm Constant
R	Ideal Gas Constant
C_o	Initial Concentration of Adsorbate in the Solution
b	Langmuir Isotherm Constant
W	Mass of Adsorbent
Q_o	Maximum Monolayer Coverage Capacity Constant at Equilibrium
MOFs	Metal-organic Frameworks
MO	Methyl Orange
NSAIDs	Nonsteroidal Anti-inflammatory Drugs
PhPy	Phenazopyridine Hydrochloride
PZC	Point of Zero Charge
SEM	Scanning Electron Microscopy
TGA	Thermogravimetric Analysis
V	Volume of Aqueous Solution
XRD	X-Ray Diffraction

References

1. The Noble Quran: English Translation of the Meanings and Commentary. Riyadh (Saudi Arabia): King Fahd Complex. 1997.
2. Lorenzo I, Serra-Prat M, Yebenes JC. The Role of Water Homeostasis in Muscle Function and Frailty: A Review. Nutrients. 2019;11(8).
3. Sensoy I. A review on the food digestion in the digestive tract and the used in vitro models. Curr Res Food Sci. 2021;4:308-19.
4. Frank AW, M P-V. Water conservation in irrigation can increase water use. The National Academy of Sciences. 2008;47:215-20.
5. Hodges M, Belle JH, Carlton EJ, Liang S, Li H, Luo W, et al. Delays reducing waterborne and water-related infectious diseases in China under climate change. Nat Clim Chang. 2014;4:1109-15.
6. Vorosmarty CJ, McIntyre PB, Gessner MO, Dudgeon D, Prusevich A, Green P, et al. Global threats to human water security and river biodiversity. Nature. 2010;467(7315):555-61.
7. Steffen W, Richardson K, Rockstrom J, Cornell SE, Fetzer I, Bennett EM, et al. Sustainability. Planetary boundaries: guiding human development on a changing planet. Science. 2015;347(6223):1259855.
8. Myung K, Madary MW, Satchivi NM. A simple method to determine mineralization of (14) C-labeled compounds in soil. Environ Toxicol Chem. 2014;33(6):1303-7.
9. Djebbar M, Djafri F, Bouchekara M, Djafri A. Adsorption of phenol on natural clay. Applied Water Science. 2012;2(2):77-86.
10. Karimi-Maleh H, Shafieizadeh M, Taher MA, Opoku F, Kiarii EM, Govender PP, et al. The role of magnetite/graphene oxide nano-composite as a high-efficiency adsorbent for removal of phenazopyridine residues from water samples, an experimental/theoretical investigation. Journal of Molecular Liquids. 2020;298.
11. Feng Y, yang l, Liu J, Logan B. Electrochemical Technologies for Wastewater Treatment and Resource Reclamation. Environ Sci: Water Res Technol. 2016;2.

12. Carlos L, Garcia Einschlag FS, C M, O D. Applications of Magnetite Nanoparticles for Heavy Metal Removal from Wastewater. Waste Water - Treatment Technologies and Recent Analytical Developments2013.

13. Hsin w. Adsorption of Reactive Dye Onto Carbon Nanotubes: Equilibrium, Kinetics and Thermodynamics. Journal of hazardous materials. 2007;144:93-100.

14. Toth J. Adsorption: CRC Press; 2002.

15. Nassar Nashaat N. The application of nanoparticles for wastewater remediation. Applications of Nanomaterials for Water Quality2013. p. 52-65.

16. Qu M, Liu G, Zhao J, Li H, Liu W, Yan Y, et al. Fate of atrazine and its relationship with environmental factors in distinctly different lake sediments associated with hydrophytes. Environ Pollut. 2020;256:113371.

17. Fletcher TD, Shuster W, Hunt WF, Ashley R, Butler D, Arthur S, et al. SUDS, LID, BMPs, WSUD and more – The evolution and application of terminology surrounding urban drainage. Urban Water Journal. 2014;12(7):525-42.

18. Singh MR, Gupta A. Water pollution-sources, effects and control. Centre for Biodiversity, Department of Botany, Nagaland University. 2016:1-16.

19. Oller I, Malato S, Sánchez-Pérez JA. Combination of Advanced Oxidation Processes and biological treatments for wastewater decontamination--a review. Sci Total Environ. 2011;409(20):4141-66.

20. Gürses A, Açıkyıldız M, Güneş K, Gürses MS, Gürses A, Açıkyıldız M, et al. Dyes and pigments: their structure and properties. Dyes and pigments. 2016:13-29.

21. dos Santos AB, Cervantes FJ, van Lier JB. Review paper on current technologies for decolourisation of textile wastewaters: perspectives for anaerobic biotechnology. Bioresour Technol. 2007;98(12):2369-85.

22. Al Prol AE. Study of environmental concerns of dyes and recent textile effluents treatment technology: a review. Asian Journal of Fisheries and Aquatic Research. 2019;3(2):1-18.

23. Pinheiro HM, Touraud E, Thomas O. Aromatic amines from azo dye reduction: status review with emphasis on direct UV spectrophotometric detection in textile industry wastewaters. Dyes and Pigments. 2004;61(2):121-39.

24. Waring DR, Hallas G, editors. The chemistry and application of dyes1990.

25. Rauf MA, Ashraf SS. Fundamental principles and application of heterogeneous photocatalytic degradation of dyes in solution. Chemical Engineering Journal. 2009;151(1-3):10-8.

26. Pandey A, Singh P, Iyengar L. Bacterial Decolorization and Degradation of Azo Dyes. International Biodeterioration & Biodegradation. 2007;59:73-84.

27. Barciela P, Perez-Vazquez A, Prieto MA. Azo dyes in the food industry: Features, classification, toxicity, alternatives, and regulation. Food Chem Toxicol. 2023;178:113935.

28. Alzain H, Kalimugogo V, Hussein K. A Review of Environmental Impact of Azo Dyes. International Journal of Research and Review. 2023;10(6):64-689.

29. Benkhaya S, M'Rabet S, El Harfi A. Classifications, properties, recent synthesis and applications of azo dyes. Heliyon. 2020;6(1):e03271.

30. Yao Y, Bing H, Feifei X, Xiaofeng C. Equilibrium and kinetic studies of methyl orange adsorption on multiwalled carbon nanotubes. Chemical Engineering Journal. 2011;170(1):82-9.

31. Mittal A, Malviya A, Kaur D, Mittal J, Kurup L. Studies on the adsorption kinetics and isotherms for the removal and recovery of Methyl Orange from wastewaters using waste materials. Journal of hazardous materials. 2007;148(1-2):229-40.

32. Guin JP, Bhardwaj Y, Varshney L. Mineralization and biodegradability enhancement of Methyl Orange dye by an effective advanced oxidation process. Applied Radiation and Isotopes. 2017;122:153-7.

33. Sejie FP, Nadiye-Tabbiruka MS. Removal of methyl orange (MO) from water by adsorption onto modified local clay (kaolinite). Physical Chemistry. 2016;6(2):39-48.

34. Hughes SR, Kay P, Brown LE. Global synthesis and critical evaluation of pharmaceutical data sets collected from river systems. Environ Sci Technol. 2013;47(2):661-77.

35. López-Serna R, Petrović M, Barceló D. Occurrence and distribution of multi-class pharmaceuticals and their active metabolites and transformation products in the Ebro river basin (NE Spain). Sci Total Environ. 2012;440:280-9.

36. Singer AC, Shaw H, Rhodes V, Hart A. Review of Antimicrobial Resistance in the Environment and Its Relevance to Environmental Regulators. Front Microbiol. 2016;7:1728.

37. Kidd KA, Blanchfield PJ, Mills KH, Palace VP, Evans RE, Lazorchak JM, et al. Collapse of a fish population after exposure to a synthetic estrogen. Proc Natl Acad Sci U S A. 2007;104(21):8897-901.

38. Ternes TA. Occurrence of drugs in German sewage treatment plants and rivers1Dedicated to Professor Dr. Klaus Haberer on the occasion of his 70th birthday.1. Water Research. 1998;32(11):3245-60.

39. Cleuvers M. Aquatic ecotoxicity of pharmaceuticals including the assessment of combination effects. Toxicol Lett. 2003;142(3):185-94.

40. Schwaiger J, Ferling H, Mallow U, Wintermayr H, Negele RD. Toxic effects of the non-steroidal anti-inflammatory drug diclofenac. Part I: histopathological alterations and bioaccumulation in rainbow trout. Aquat Toxicol. 2004;68(2):141-50.

41. Webb S, Ternes T, Gibert M, Olejniczak K. Indirect human exposure to pharmaceuticals via drinking water. Toxicol Lett. 2003;142(3):157-67.

42. Zelenitsky SA, Zhanel GG. Phenazopyridine in urinary tract infections. Annals of Pharmacotherapy. 1996;30(7-8):866-8.

43. Meegan M, O'Boyle N. Special Issue “Anticancer Drugs”. Pharmaceuticals. 2019;12:134.

44. Tao Q, Chen J-M, Ma L, Lu T-B. Phenazopyridine cocrystal and salts that exhibit enhanced solubility and stability. Crystal growth & design. 2012;12(6):3144-52.

45. Schwarzenbach RP, Egli T, Hofstetter TB, Von Gunten U, Wehrli B. Global water pollution and human health. Annual review of environment and resources. 2010;35(1):109-36.

46. Gupta VK, Suhas. Application of low-cost adsorbents for dye removal – A review. Journal of Environmental Management. 2009;90(8):2313-42.

47. Forgacs E, Cserháti T, Oros G. Removal of synthetic dyes from wastewaters: a review. Environment International. 2004;30(7):953-71.

48. Ciardelli G, Corsi L, Marcucci M. Membrane separation for wastewater reuse in the textile industry. Resources, Conservation and Recycling. 2001;31(2):189-97.

49. Chakrabarti S, Dutta BK. Photocatalytic degradation of model textile dyes in wastewater using ZnO as semiconductor catalyst. Journal of Hazardous Materials. 2004;112(3):269-78.

50. Yang X, Wan Y, Zheng Y, He F, Yu Z, Huang J, et al. Surface functional groups of carbon-based adsorbents and their roles in the removal of heavy metals from aqueous solutions: A critical review. Chemical Engineering Journal. 2019;366:608-21.

51. Thommes M, Cychosz KA. Physical adsorption characterization of nanoporous materials: progress and challenges. Adsorption. 2014;20(2):233-50.

52. Ünveren EE, Monkul BÖ, Sarıoğlan Ş, Karademir N, Alper E. Solid amine sorbents for CO2 capture by chemical adsorption: A review. Petroleum. 2017;3(1):37-50.

53. Boyd G, Schubert J, Adamson A. The exchange adsorption of ions from aqueous solutions by organic zeolites. I. Ion-exchange equilibria1. Journal of the American Chemical society. 1947;69(11):2818-29.

54. Fierro J. Structure and composition of perovskite surface in relation to adsorption and catalytic properties. Catalysis today. 1990;8(2):153-74.

55. Trickett C, Helal A, Al-maythalony B, Yamani Z, Cordova K, Yaghi O. The chemistry of metal–organic frameworks for CO2 capture, regeneration and conversion. Nature Reviews Materials. 2017;2:natrevmats201745.

56. Heidarinejad Z, Dehghani MH, Heidari M, Javedan G, Ali PI, Sillanpää M. Methods for preparation and activation of activated carbon: a review. Environmental Chemistry Letters. 2020;18:1-23.

57. Gaber D, Abu Haija M, Eskhan A, Banat F. Graphene as an efficient and reusable adsorbent compared to activated carbons for the removal of phenol from aqueous solutions. Water, Air, & Soil Pollution. 2017;228:1-14.

58. Adeyemo AA, Adeoye IO, Bello OS. Adsorption of dyes using different types of clay: a review. Applied Water Science. 2017;7:543-68.

59. Onawole AT, Nasser MS, Hussein IA, Al-Marri MJ, Aparicio S. Theoretical studies of methane adsorption on Silica-Kaolinite interface for shale reservoir application. Applied Surface Science. 2021;546:149164.

60. Armstrong NA, Clarke CD. Adsorption sites of kaolin. J Pharm Sci. 1976;65(3):373-5.

61. Gaines GL, Jr., Thomas HC. Adsorption Studies on Clay Minerals. II. A Formulation of the Thermodynamics of Exchange Adsorption. The Journal of Chemical Physics. 1953;21(4):714-8.

62. Ioannou A, Dimirkou A. Phosphate Adsorption on Hematite, Kaolinite, and Kaolinite-Hematite (k-h) Systems As Described by a Constant Capacitance Model. J Colloid Interface Sci. 1997;192(1):119-28.

63. Bouazza A. Geosynthetic clay liners. Geotextiles and Geomembranes. 2002;20(1):3-17.

64. Aboudi S, Hanafiah M, Chowdhury A. Environmental characteristics of clay and clay-based minerals. Geology, Ecology, and Landscapes. 2017;1:155-61.

65. Sinha Ray S, Okamoto M. Polymer/layered silicate nanocomposites: a review from preparation to processing. Progress in Polymer Science. 2003;28(11):1539-641.

66. Jlassi K, Krupa I, Chehimi MM. Overview: clay preparation, properties, modification. Clay-polymer nanocomposites. 2017:1-28.

67. Madejova J. Baseline Studies of the Clay Minerals Society Source Clays: Infrared Methods. Clays and Clay Minerals - CLAYS CLAY MINER. 2001;49:410-32.

68. Conceição S, Santos N, Velho J, Ferreira J. Properties of paper coated with kaolin: The influence of the rheological modifier. Applied Clay Science - APPL CLAY SCI. 2005;30:165-73.

69. Chiara Z, Raimondo M, Guarini G, Dondi M. The vitreous phase of porcelain stoneware: Composition, evolution during sintering and physical properties. Journal of Non-crystalline Solids - J NON-CRYST SOLIDS. 2011;357:3251-60.

70. Pavlidou S, Papaspyrides C. A Review on Polymer–Layered Silicate Nanocomposites. Progress in Polymer Science. 2008;33:1119-98.

71. Müller AS, Janjić K, Shokoohi-Tabrizi H, Oberoi G, Moritz A, Agis H. The response of periodontal cells to kaolinite. Clin Oral Investig. 2020;24(3):1205-15.

72. Harris RG, Johnson BB, Wells JD. Studies on the adsorption of dyes to kaolinite. Clays and clay minerals. 2006;54(4):435-48.

73. Dadebo D, Obura D. Removal of Acid Red 88 from an Aqueous Solution Using Kaolinite Clay by Adsorption Process. East African Journal of Engineering. 2022;5:57-71.

74. Ghosh D, Bhattacharyya K. Adsorption of Methylene Blue on Kaolinite. Applied Clay Science. 2002;20:295-300.

75. Vimonses V, Lei S, Jin B, Chow C, Saint C. Adsorption of congo red by three Australian kaolins. Applied Clay Science. 2009;43:465-72.

76. Onyekweli A, Usifoh C, Okunrobo L. Adsorptive property of kaolin in some drug formulations. Tropical Journal of Pharmaceutical Research (ISSN: 1596-5996) Vol 2 Num 1. 2005;2.

77. Foo KY, Hameed BH. Insights into the modeling of adsorption isotherm systems. Chemical Engineering Journal. 2010;156(1):2-10.

78. Limousin G, Gaudet J-P, Charlet L, Szenknect S, Barthès V, Krimissa M. Sorption isotherms: A review on physical bases, modeling and measurement. Applied Geochemistry. 2007;22:249-75.

79. Liu L, Lin Y, Liu Y, Zhu H, He Q. Removal of Methylene Blue from Aqueous Solutions by Sewage Sludge Based Granular Activated Carbon: Adsorption

Equilibrium, Kinetics, and Thermodynamics. Journal of Chemical & Engineering Data. 2013;58:2248–53.

80. Wahyuni N, Zissis G, Mouloungui Z. Characterization of acid sites on modified kaolinite by FTIR spectra of pyridine adsorbed2018. 020042 p.

81. Zyoud AH, Zubi A, Zyoud SH, Hilal MH, Zyoud S, Qamhieh N, et al. Kaolin-supported ZnO nanoparticle catalysts in self-sensitized tetracycline photodegradation: Zero-point charge and pH effects. Applied Clay Science. 2019;182:105294.

82. Mayerhöfer TG, Popp J. Beer's Law–why absorbance depends (almost) linearly on concentration. ChemPhysChem. 2019;20(4):511-5.

83. Lothenbach B, Durdzinski P, De Weerdt K. Thermogravimetric analysis. A practical guide to microstructural analysis of cementitious materials. 2016;1:177-211.

84. Xu H, Van Deventer JS. Microstructural characterisation of geopolymers synthesised from kaolinite/stilbite mixtures using XRD, MAS-NMR, SEM/EDX, TEM/EDX, and HREM. Cement and Concrete research. 2002;32(11):1705-16.

85. Faqir N, Shawabkeh R, Al-Harthi M, Al-Abdul Wahhab H. Fabrication of Geopolymers from Untreated Kaolin Clay for Construction Purposes. Geotechnical and Geological Engineering. 2019;37.

86. Tironi A, Trezza MA, Irassar EF, Scian AN. Thermal Treatment of Kaolin: Effect on the Pozzolanic Activity. Procedia Materials Science. 2012;1:343-50.

87. Revellame ED, Fortela DL, Sharp W, Hernandez R, Zappi ME. Adsorption kinetic modeling using pseudo-first order and pseudo-second order rate laws: A review. Cleaner Engineering and Technology. 2020;1:100032.

88. Wang J, Guo X. Adsorption kinetic models: Physical meanings, applications, and solving methods. Journal of Hazardous materials. 2020;390:122156.

89. Simonin J-P, Bouté J. Intraparticle diffusion-adsorption model to describe liquid/solid adsorption kinetics. Revista mexicana de ingeniería química. 2016;15(1):161-73.

90. Rodda DP, Johnson BB, Wells JD. Modeling the Effect of Temperature on Adsorption of Lead(II) and Zinc(II) onto Goethite at Constant pH. Journal of Colloid and Interface Science. 1996;184(2):365-77.

91. Eren E. Removal of lead ions by Unye (Turkey) bentonite in iron and magnesium oxide-coated forms. Journal of Hazardous Materials. 2009;165(1):63-70.

92. Sarkar M, Acharya PK, Bhattacharya B. Modeling the adsorption kinetics of some priority organic pollutants in water from diffusion and activation energy parameters. Journal of colloid and interface science. 2003;266(1):28-32.

93. Nassar NN. Rapid removal and recovery of Pb(II) from wastewater by magnetic nanoadsorbents. Journal of Hazardous Materials. 2010;184(1):538-46.

94. Aljamali NM, Khdur R, Alfatlawi IO. Physical and chemical adsorption and its applications. International Journal of Thermodynamics and Chemical Kinetics. 2021;7(2):1-8.

95. Attia K, El-Abasawi N, El-Olemy A, Abdelazim A. Comparative Study of Different Spectrophotometric Methods for Determination of Phenazopyridine Hydrochloride in the Presence of its Oxidative Degradation Product. Analytical Chemistry Letters. 2016;6:863-73.

96. Cyril N, George J, Joseph L, Sylas V. Catalytic Degradation of Methyl Orange and Selective Sensing of Mercury Ion in Aqueous Solutions Using Green Synthesized Silver Nanoparticles from the Seeds of Derris trifoliata. Journal of Cluster Science. 2019;30.

Appendices

Appendix A1

Figures

Figure A.1

Adsorption of PhPy on modified kaolinite at different temperatures, pH of 5, and shaking speed of 200 rpm for half an hour: (a) 0.2 g/50 mL for 30 ppm and (b) 0.5 g/50 mL for 60 ppm

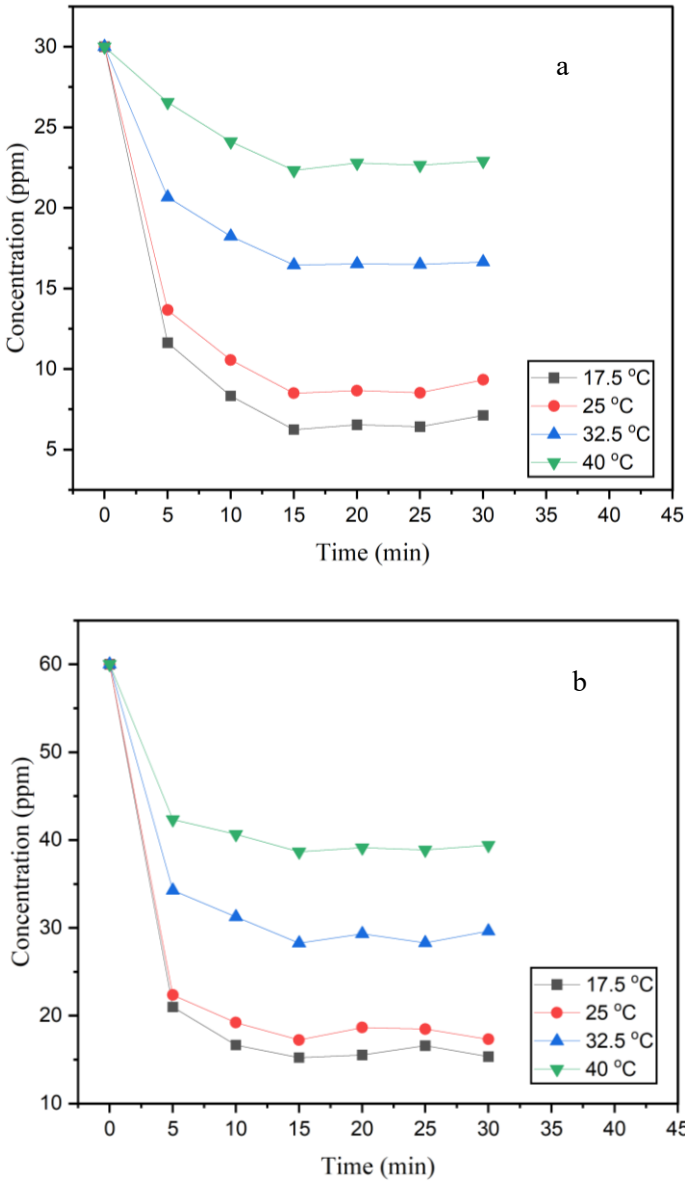

Figure A.2

Plot of 1/T vs Ln k to determine the activation energy for the adsorption of PhPy on modified kaolinite

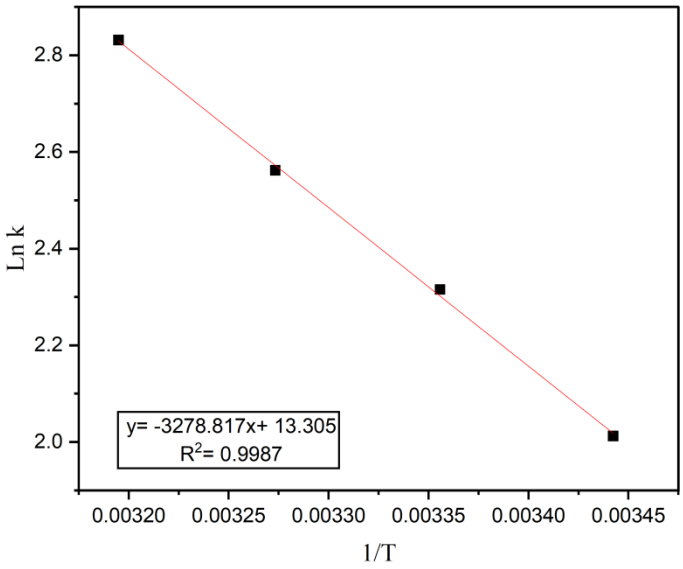

Figure A.3

TGA results of modified kaolinite and PhPy

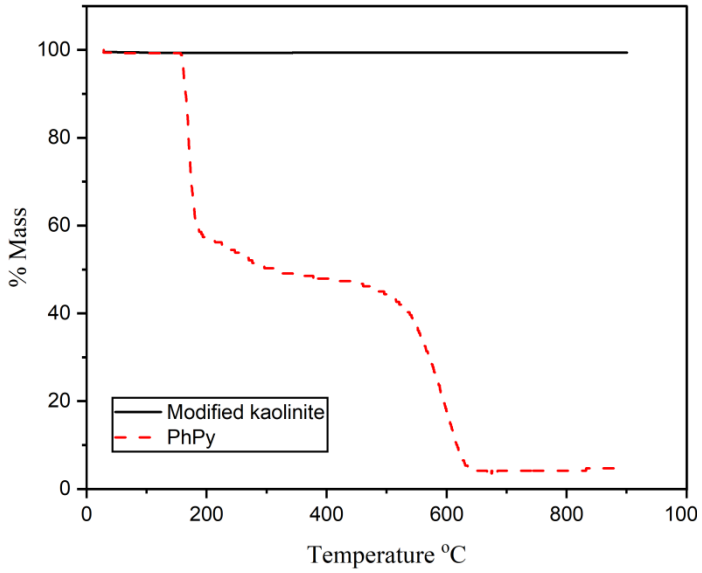

Figure A.4

Stability of modified kaolinite after reuse, % removal of PhPy for the 4 reuse experiments

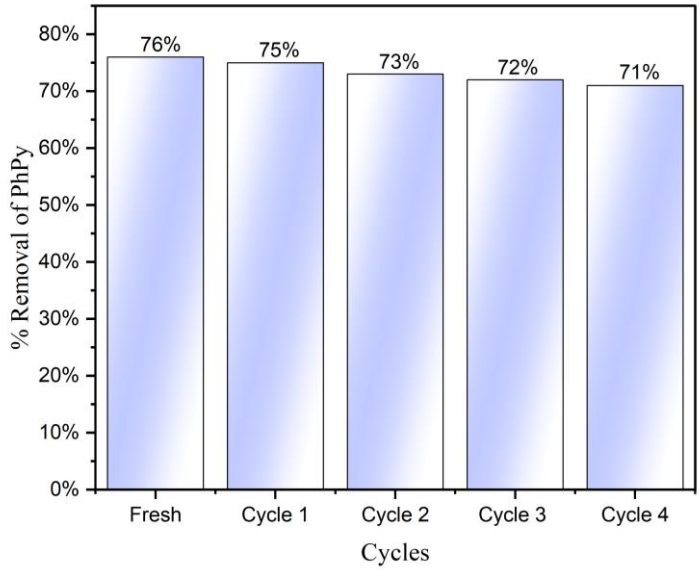

Figure A.5

FTIR spectra for PhPy adsorption onto modified kaolinite: (a) pure modified kaolinite, (b) PhPy (c) PhPy onto modified kaolinite (d) PhPy onto modified kaolinite after thermal decomposition at 600 °C

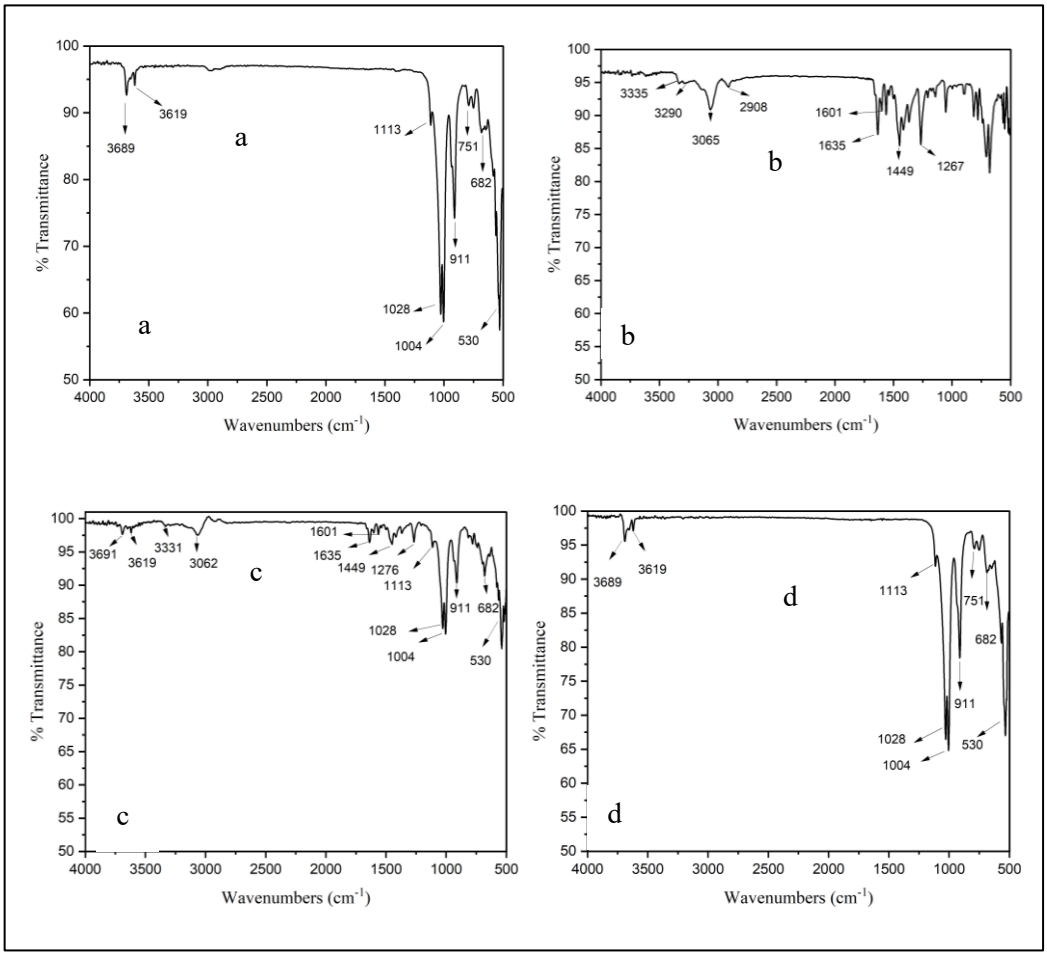

Figure A.6

Calibration curve of MO

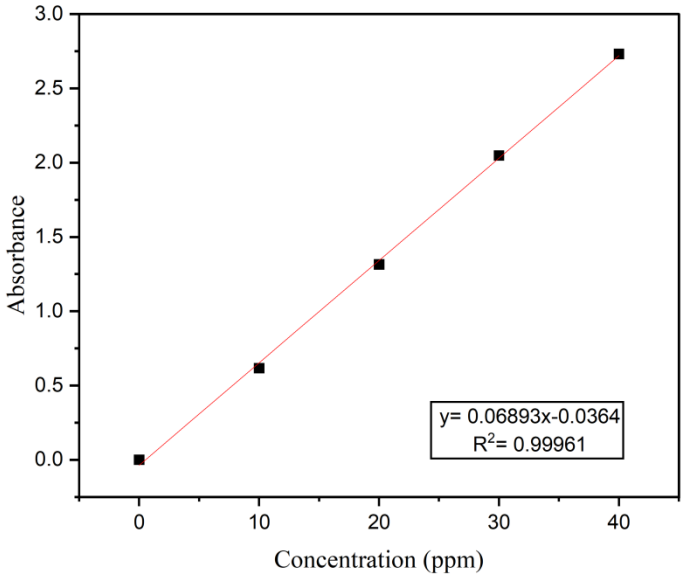

Figure A.7

Amounts of MO removed (ppm) over time under various conditions, 0.5 g/50 mL, pH of 2, shaking speed of 200 rpm and 25 °C for half an hr

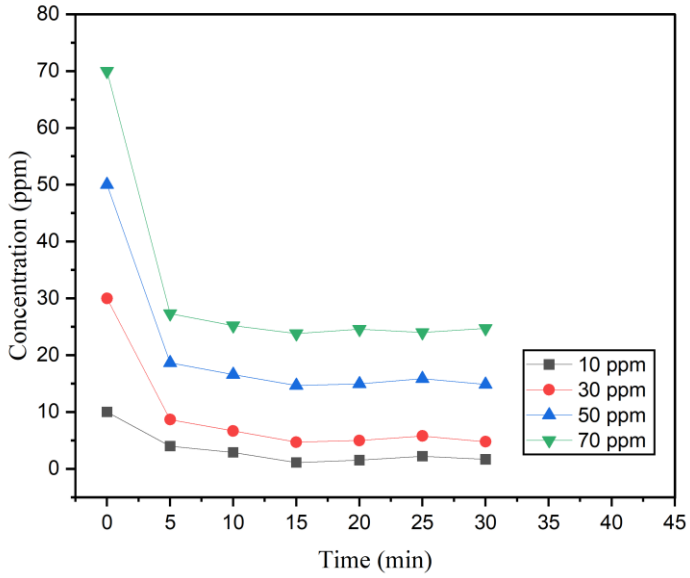

Figure A.8

Effect of the amount of adsorbent (g) on the removal efficiency of MO. Conditions, 50 mL of MO solution (50 ppm), solution pH of 2, shaking time = half an hour, shaking speed = 200 rpm, and 25 °C.

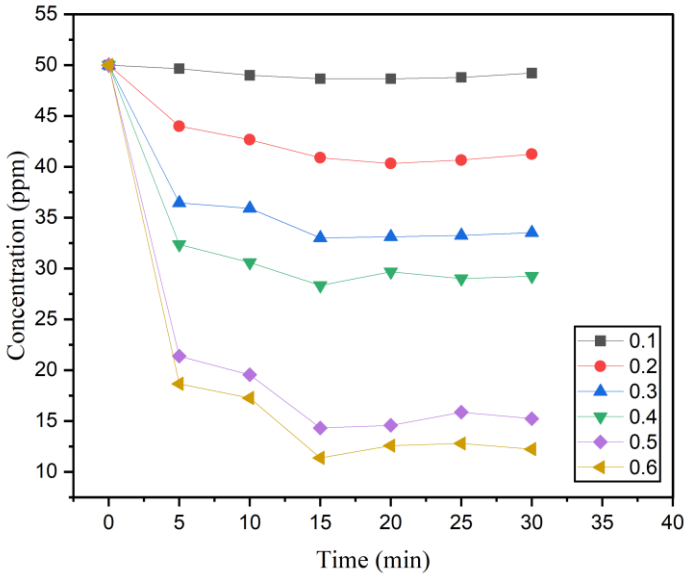

Figure A.9

Effect of pH on the removal efficiency of MO. The conditions used were as follows: 50 mL of MO solution (50 ppm), shaking time is half an hour, amount of adsorbent is 0.5 g, shaking speed is 200 rpm, and 25 °C

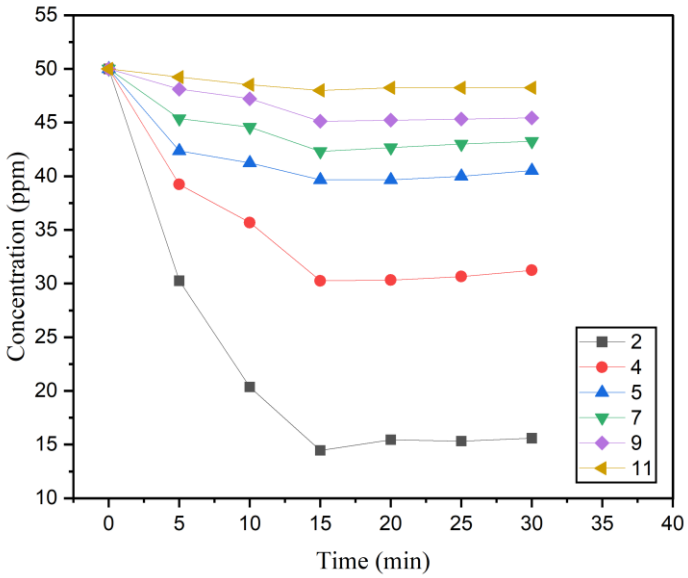

Figure A.10

(a) Adsorption isotherms of MO onto modified kaolinite, (b) Langmuir isotherm, and (c) Freundlich isotherm.

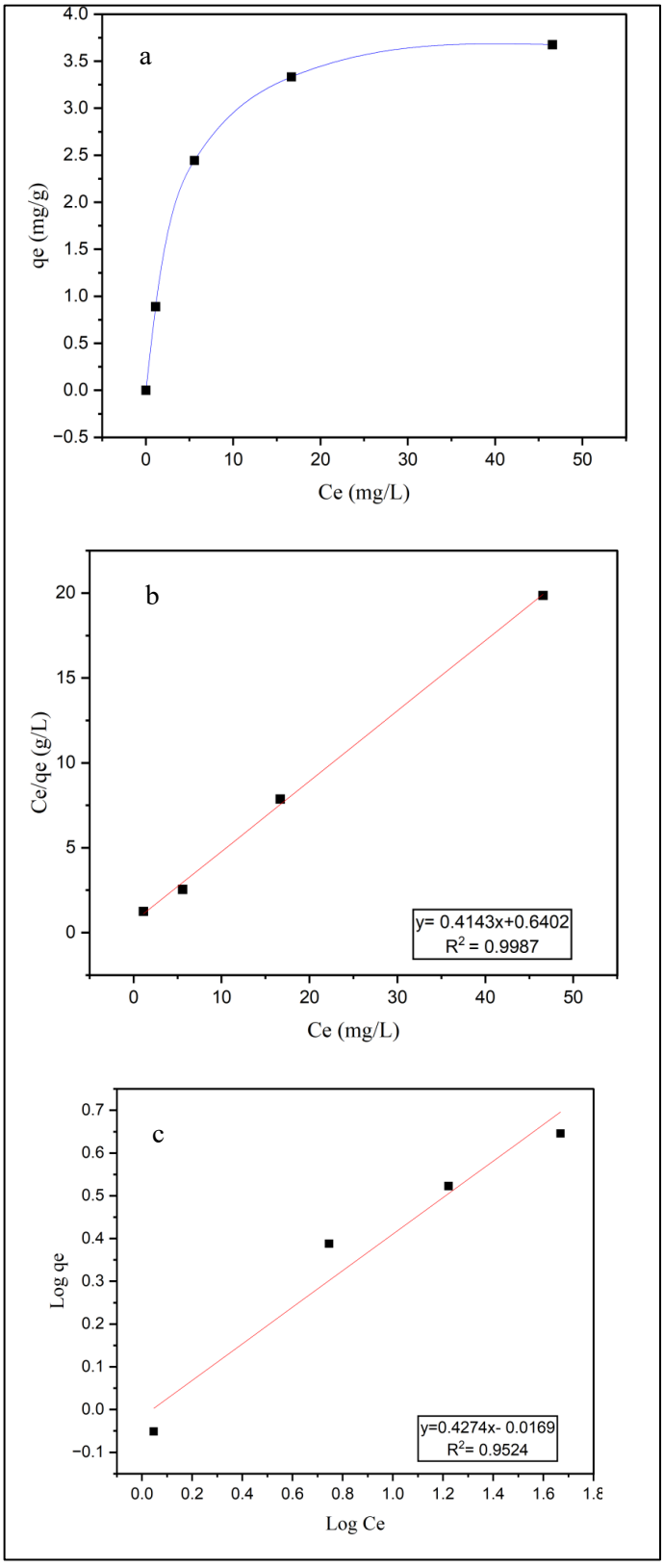

Figure A.11

(a) Pseudo first-order, (b) Pseudo second-order, and (c) Intra particle diffusion

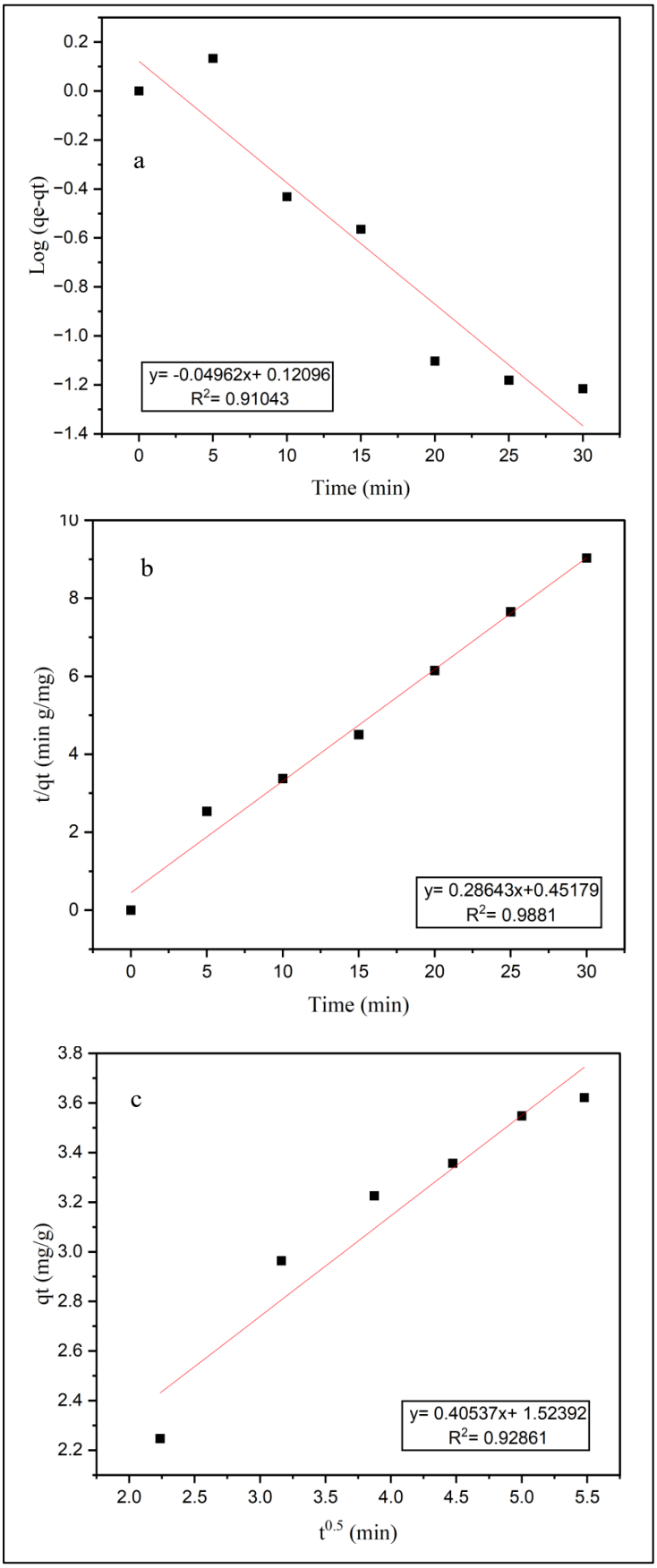

Figure A.12

Adsorption of MO on modified kaolinite at different temperatures, pH of 2, and shaking speed of 200 rpm for half an hour at 0.5 g/50 mL

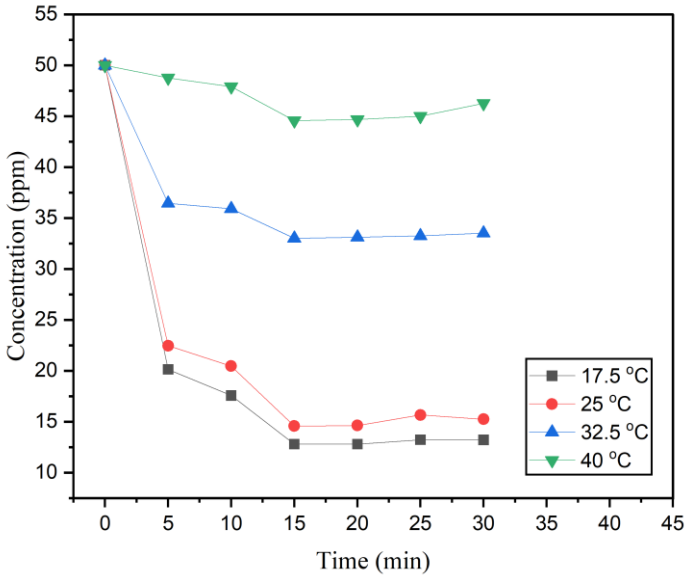

Figure A.13

Plot of 1/T vs Ln k to determine the activation energy for the adsorption of MO on modified kaolinite

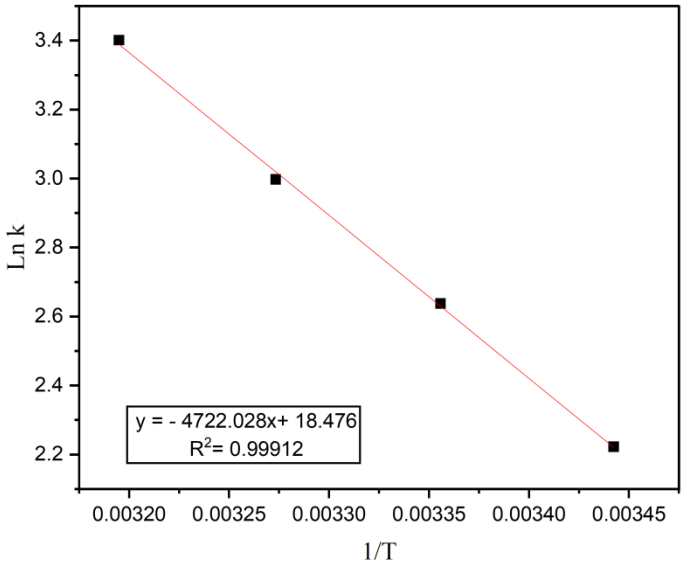

Figure A.14

TGA results of modified kaolinite and MO

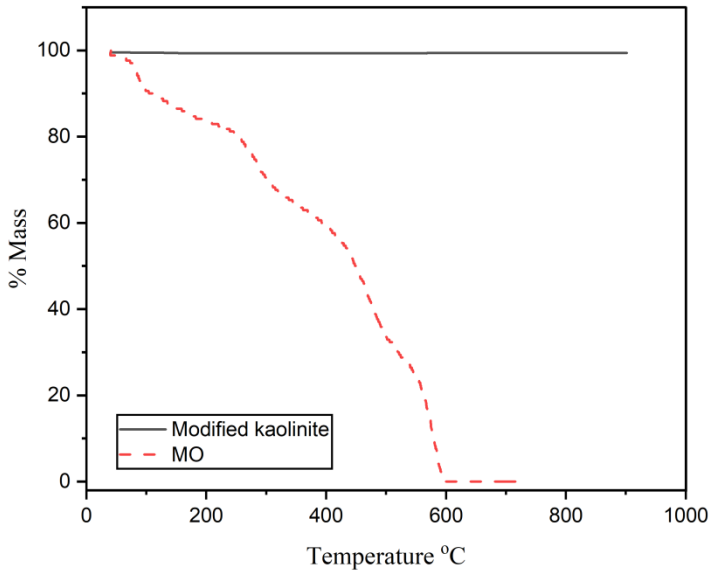

Figure A.15

Stability of modified kaolinite after reuse, % removal of MO for the 4 reuse experiments

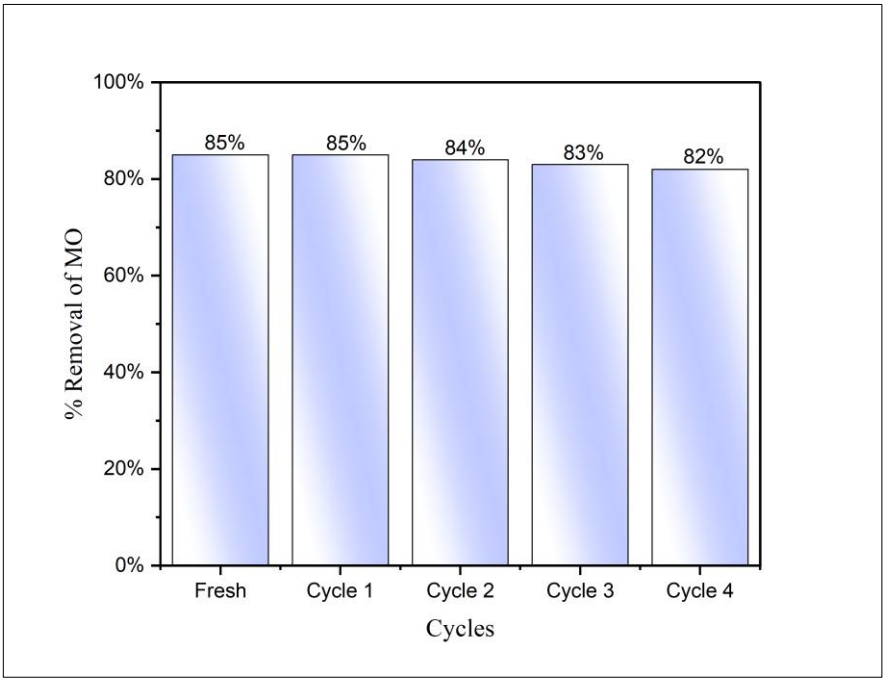

Figure A.16

FTIR spectra for MO adsorption onto modified kaolinite: (a) pure modified kaolinite, (b) MO (c) MO onto modified kaolinite (d) MO onto modified kaolinite after thermal decomposition at 600 °C

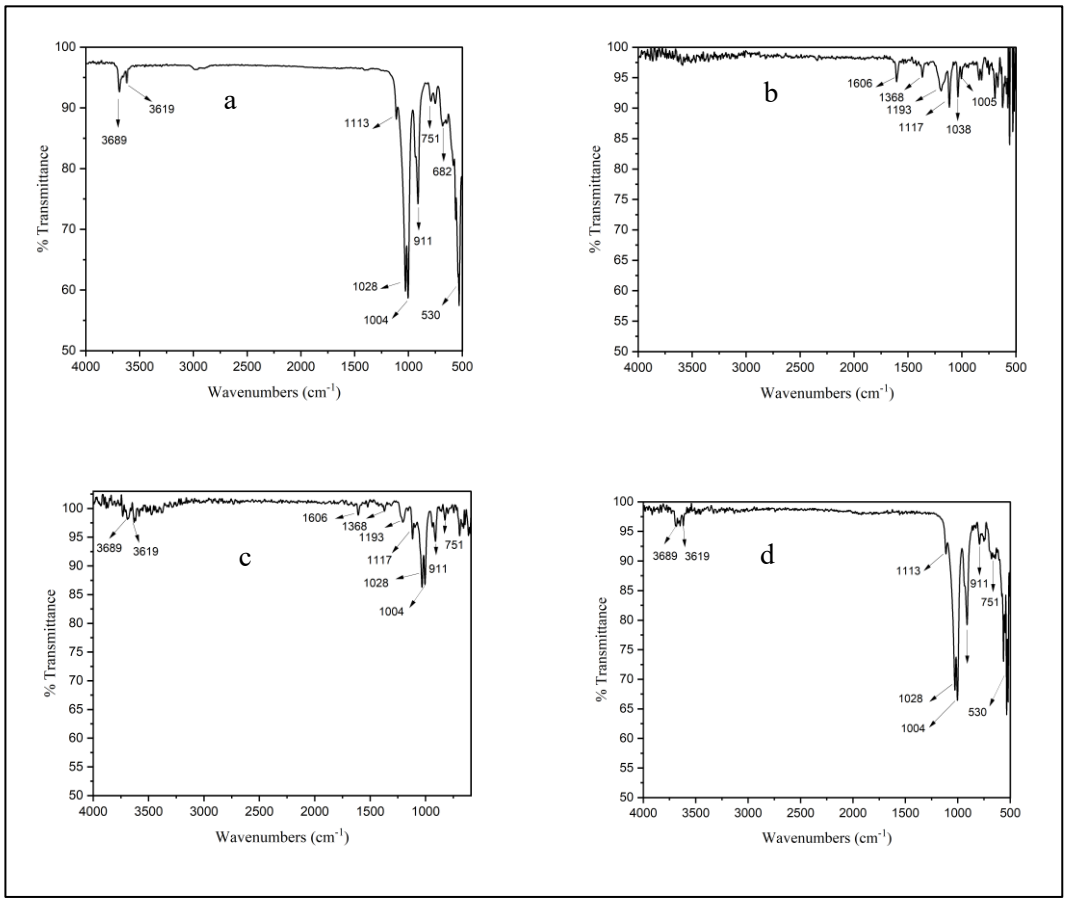

جامعة النجاح الوطنية

كلية الدراسات العليا

الكولينايت لإزالة الفينازوبريدين من المياه الملوثة عن طريق الامتزاز متبوعاً بتقنية التحلل الحراري

إعداد

سهر مرزوق عبد الرحمن سلمان

إشراف

أ.د عاهد زيود

د. ضرار الصمادي

قدمت هذه الأطروحة استكمال لمتطلبات الحصول على درجة الماجستير في الكيمياء بكلية الدراسات العليا في جامعة النجاح الوطنية، نابلس- فلسطين

2024

الكولينايت لإزالة الفينازوبريدين من المياه الملوثة عن طريق الامتزاز متبوعاً بتقنية التحلل الحراري

إعداد

سهر مرزوق عبد الرحمن سلمان

إشراف

أ.د عاهد زيود

د. ضرار الصمادي

الملخص

في هذه الدراسة، تم استخدام الكاولينايت المعدل كمادة ماصة لإزالة صبغات الفينازوبيريدين هيدروكلوريد والميثل أورانج من المحلول المائي. تم تحليل تأثير تراكيز المادة الملوثة، كمية الكاولينايت المعدل، الرقم الهيدروجيني، ودرجة الحرارة باستخدام UV-Vis. لوحظ أن الامتزاز يزداد بانخفاض التركيز ويصل للتوازن مع كمية معينة من الكاولينايت المعدل.

الرقم الهيدروجيني الأمثل لامتزاز الفينازوبيريدين هيدروكلوريد كان 5، بينما للميثل أورانج كان 2، مع تحقيق التوازن خلال 15 دقيقة. الامتزاز كان طاردًا للحرارة حيث تناقصت الكميات الممتزة مع زيادة درجة الحرارة. تبعت حركية الامتزاز نموذج Pseudo-second order، وتوافقت البيانات التجريبية مع نموذج لانغمير لكلا الصبغتين. تم تحليل الامتزاز باستخدام معادلة أرهينيوس وحُسبت طاقة التنشيط، مما أشار إلى امتزاز فيزيائي.

وللتعرف على الخصائص الامتزازية للكاولينايت المعدل، استُخدم حيود الأشعة السينية (XRD) لتحديد التركيب البلوري وتأكيد التعديل الناجح. كشفت أنماط XRD تغييرات في تباعد الطبقات البينية، مما يدل على التفاعل بين الكاولينايت و$ZnCl_2$. أظهرت صور المجهر الإلكتروني الماسح (SEM) زيادة في خشونة السطح والمسامية. قياس الحرارة الحراري (TGA) كشف عن ثبات حراري ممتاز للكاولينايت المعدل، مع استمراره حتى درجات حرارة مرتفعة، مما يضمن إمكانية تجديده لأربع دورات من خلال التحلل الحراري عند 600 درجة مئوية دون فقد كفاءة الامتزاز.أظهر التحليل الطيفي بالأشعة تحت الحمراء (FT-IR) تغييرات في اهتزازات مجموعات وظيفية، مما أكد امتزاز PhPy وMO على سطح الكاولينايت المعدل. بعد المعالجة

الحرارية عند 600 درجة مئوية، كشفت أطياف FT-IR عن اختفاء القمم المرتبطة بالمجموعات الوظيفية للأصباغ، مما يثبت التحلل الناجح وإعادة تأهيل الكاولينايت للاستخدام.

الكلمات المفتاحية: الكاولينيت المعدل، فينازوبيريدين هيدروكلوريد، ميثيل أورانج، الامتزاز، المعالجة الحرارية.